

INTEGRAL/IBIS nine-year Galactic Hard X-Ray Survey*

R. Krivonos^{1,2}, S. Tsygankov^{3,4,2}, A. Lutovinov², M. Revnivtsev², E. Churazov^{1,2}, R. Sunyaev^{1,2}

¹ Max-Planck-Institut für Astrophysik, Karl-Schwarzschild-Str. 1, D-85740 Garching bei München, Germany

² Space Research Institute, Russian Academy of Sciences, Profsoyuznaya 84/32, 117997 Moscow, Russia

³ Finnish Centre for Astronomy with ESO (FINCA), University of Turku, Väisäläntie 20, FI-21500 Piikkiö, Finland

⁴ Astronomy Division, Department of Physics, FI-90014 University of Oulu, Finland

Preprint online version: September 17, 2018

ABSTRACT

Context. The INTEGRAL observatory operating in a hard X-ray/gamma domain has gathered a large observational data set over nine years starting in 2003. Most of the observing time was dedicated to the Galactic source population study, making possible the deepest Galactic survey in hard X-rays ever compiled.

Aims. We aim to perform a Galactic survey that can be used as the basis of Galactic source population studies, and perform mapping of the Milky Way in hard X-rays over the maximum exposure available at $|b| < 17.5^\circ$.

Methods. We used sky reconstruction algorithms especially developed for the high quality imaging of INTEGRAL/IBIS data.

Results. We present sky images, sensitivity maps, and catalogs of detected sources in the three energy bands $17 - 60$, $17 - 35$, and $35 - 80$ keV in the Galactic plane at $|b| < 17.5^\circ$. The total number of sources in the reference $17 - 60$ keV band includes 402 objects exceeding a 4.7σ detection threshold on the nine-year time-averaged map. Among the identified sources with known and tentatively identified natures, 253 are Galactic objects (108 low-mass X-ray binaries, 82 high-mass X-ray binaries, 36 cataclysmic variables, and 27 are of other types), and 115 are extragalactic objects, including 112 active galactic nuclei (AGNs) and 3 galaxy clusters. The sample of Galactic sources with $S/N > 4.7\sigma$ has an identification completeness of $\sim 92\%$, which is valuable for population studies. Since the survey is based on the nine-year sky maps, it is optimized for persistent sources and may be biased against finding transients.

Key words. Surveys – X-rays: general – Catalogs

1. Introduction

A large fraction of astrophysical phenomena cannot be studied via observations of individual sources, but require instead large statistical studies. The last few decades have provided us with great opportunities for studies of the populations of compact sources (black holes, neutron stars, white dwarfs) in our Galaxy and nearby galaxies.

In particular, surveys of the sky in hard X-rays were performed with the IBIS telescope (Ubertini et al., 2003) of the INTEGRAL observatory (Winkler et al., 2003) and Burst Alert Telescope (BAT; Barthelmy et al., 2005) at the *Swift* observatory (Gehrels et al., 2004). In contrast to *Swift*, with a nearly uniform all-sky survey, which is especially useful for studies of active galactic nuclei (AGN; Tueller et al., 2010; Cusumano et al., 2010; Ajello et al., 2012), the INTEGRAL observatory provides a sky survey with exposure that are deeper in the Galactic plane (GP) and has higher angular resolution, which is essential in these crowded regions. This makes the *Swift*/BAT and INTEGRAL/IBIS surveys complementary to each other.

The INTEGRAL observatory has been successfully operating in orbit since its launch in 2002. Over the past few years, INTEGRAL data has allowed us to construct high quality catalogs (Revnivtsev et al., 2004b, 2006; Molkov et al., 2004; Krivonos et al., 2005, 2007b, 2010b; Bird et al., 2006, 2007,

2010), to reveal new types of sources (Courvoisier et al., 2003; Revnivtsev et al., 2003d; Sguera et al., 2006), to calculate the statistics of active galactic nuclei (Sazonov et al., 2007; Bassani et al., 2006; Beckmann et al., 2009), of low mass X-ray binaries (Revnivtsev et al., 2008a), of high mass X-ray binaries (Lutovinov et al., 2005b, 2007; Bodaghee et al., 2007, 2012), and of cataclysmic variables (Revnivtsev et al., 2008b; Scaringi et al., 2010).

In our previous papers (Krivonos et al., 2010a,b), we presented the seven-year hard X-ray all-sky survey in the energy range $17 - 60$ keV based on the improved sky reconstruction method for the IBIS telescope. The sensitivity of the survey was significantly improved by suppressing the systematic noise.

Here we present the selected nine-year averaged sky images, sensitivity maps, and catalog of the sources detected in the Galactic plane ($|b| < 17.5^\circ$) in three energy bands: $17 - 60$, $17 - 35$, and $35 - 80$ keV. This survey is the most sensitive X-ray survey of the Galaxy existing so far and it can be used as: 1) a basis for statistical studies of different types of sources in our Galaxy, and 2) a guiding line for new surveys of a new generation of hard X-ray focusing telescopes (e.g. NuSTAR described in Harrison et al. (2010), and Astro-H in Takahashi et al. (2010)).

The full set of sky maps is available at the SkyView Virtual Observatory¹ (McGlynn et al., 1998) and Russian Science Data Center² for the INTEGRAL observatory at the Space Research Institute (IKI), Moscow.

* Based on observations with INTEGRAL, an ESA project with instruments and science data centre funded by ESA member states (especially the PI countries: Denmark, France, Germany, Italy, Switzerland, Spain), Czech Republic, and Poland, and with the participation of Russia and the USA

¹ <http://skyview.gsfc.nasa.gov>

² <http://hea.iki.rssi.ru/integral>

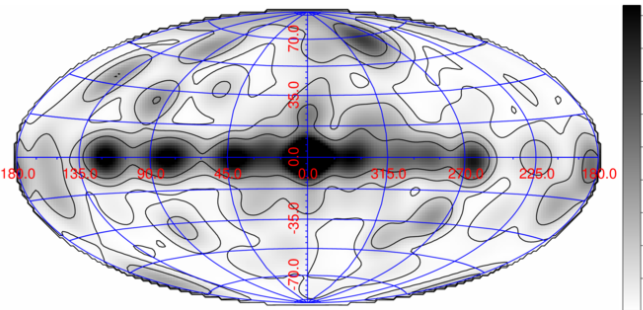


Fig. 1. Dead time-corrected exposure map of the INTEGRAL all-sky survey (January 2011, public data). The grid gap in the Galactic latitude is 17.5° , which is a half-height of the current Galactic survey. Blue contours represent exposure levels of 10, 150, 800, 2000, and 4000 ks. The effective exposure in the GC region is 12 Ms, which corresponds to 26 Ms of a nominal time.

2. Survey

To conduct the current Galactic survey, we selected publicly available INTEGRAL data from December 2002 to January 2011 (spacecraft revolutions 26–1013). Every individual INTEGRAL observation with typical exposure time of 2 ks (so called *Science Window*, *ScW*) was analyzed with a specially developed software package (see e.g. Krivonos et al. 2010a and references therein) to produce sky images in three energy bands: 17 – 60, 17 – 35, and 35 – 80 keV. In contrast to our previous surveys, the flux scale in each *ScW* sky image was adjusted using the flux of the Crab nebula measured in the nearest observations. This procedure was used to account for the ongoing detector degradation and loss of sensitivity at low energies.

In total, we obtained 73489 sky images in each band, which comprises ~ 132 Ms of the effective (dead time-corrected) exposure. The survey sky mapping was organized in six overlapping $70^\circ \times 35^\circ$ Galactic cartesian projections centered on zero Galactic latitude ($b = 0^\circ$) and $l = 0^\circ, \pm 50^\circ, \pm 115^\circ$, and $l = 180^\circ$. The latitude coverage of the survey $|b| < 17.5^\circ$ was chosen with the IBIS/ISGRI field of view ($28^\circ \times 28^\circ$) and standard $5^\circ \times 5^\circ$ observational pattern in mind. Thus, we used all observations performed by INTEGRAL in the Galactic plane. Fig. 1 illustrates the INTEGRAL exposure map of publicly available observations up to January 2011.

The survey sky coverage versus the 4.7σ limiting flux is shown in Fig. 2. The peak sensitivity of the survey is 2.9×10^{-12} erg s $^{-1}$ cm $^{-2}$ (~ 0.20 mCrab in 17–60 keV) at a 4.7σ detection level. The survey covers 90% of the geometrical area (12680 degrees) down to the flux limit of 2.0×10^{-11} erg s $^{-1}$ cm $^{-2}$ (~ 1.41 mCrab) and 10% of the total area down to the flux limit of 4.9×10^{-12} erg s $^{-1}$ cm $^{-2}$ (~ 0.30 mCrab).

2.1. Systematic noise

INTEGRAL/IBIS deep sky mosaics are usually affected by a systematic noise caused by the source confusion in the region of GC and by the imperfect sky reconstruction (Krivonos et al., 2010a).

The large field of view (FOV) of the INTEGRAL/IBIS telescope leads to a high probability of having some bright X-ray source within the instrument FOV during any galactic observations. Therefore, to work at the level of Poisson noise, the INTEGRAL/IBIS telescope image reconstruction procedure

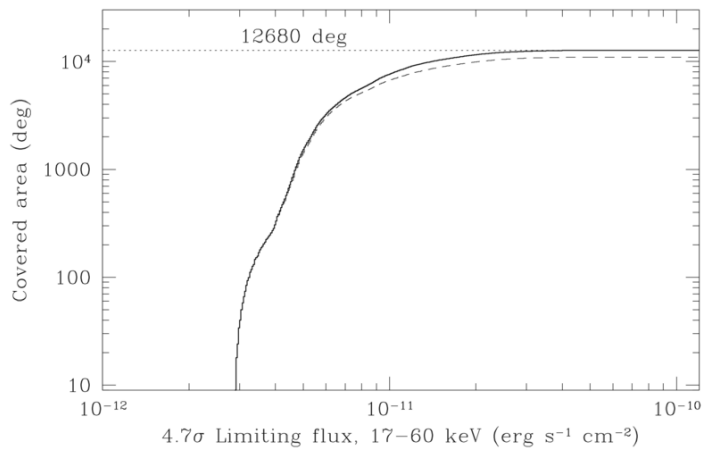


Fig. 2. Sky area as a function of the limiting flux for source detection with a 4.7σ significance (solid line). The black dashed curve shows the sky coverage with the masked area around bright sources listed in Table 1. The dotted line represents the geometrical area.

Table 1. Exclusion radius around bright sources.

Name	Exclusion radius, deg.
Crab	23.2
Sco X-1	14.0
Cyg X-1	4.8
Cyg X-3	3.9
Vela X-1	3.3
GX 301-2	2.2
GRS 1915+105	3.2

should have a dynamic range of 10^3 and more, which is very difficult to achieve owing to the imperfect modelling of the mask shadow, the individual pixel sensitivity, the variability of the background pattern, etc.

In spite of the latest version of the IBIS sky image reconstruction allowing us to reach the dynamic range of the images $\sim 10^3$, some sky artefacts are still present around bright sources, such as Crab, Sco X-1, Cyg X-1, Cyg X-3, Vela X-1, GX 301-2, and GRS 1915+105 (see a sky mosaic at $l = +50^\circ$ in Fig. 3). To prevent any false detections, we masked out circular regions around bright sources with radii listed in Table 1. The exclusion radius was chosen to contain all significant ($> 4.7\sigma$) negative excesses (indicators of the systematic noise, which is assumed to be symmetric) around a given bright source. We note that known sources with $S/N > 10\sigma$ falling inside these regions were included in the source catalog. A rejection of areas with high systematic noise significantly improved the quality of the survey mosaics, which is demonstrated in Fig. 4, where we show a distribution of signal-to-noise (S/N) values for pixels in the sky mosaic at $l = +50^\circ$. As seen from Fig. 4, the masked sky image does not contain strong deviations from the Gaussian distribution, in contrast to the original one. Masked areas around bright sources reduce the geometrical area of the survey by 13% (Fig. 2).

Systematic effects are less important in the harder energy bands. Fig. 5 shows that a sky image of the GC region in the 35 – 80 keV energy range is practically free of the systematic noise with respect to 17 – 60 keV band, which is confirmed by the S/N distribution of image pixels in Fig. 6.

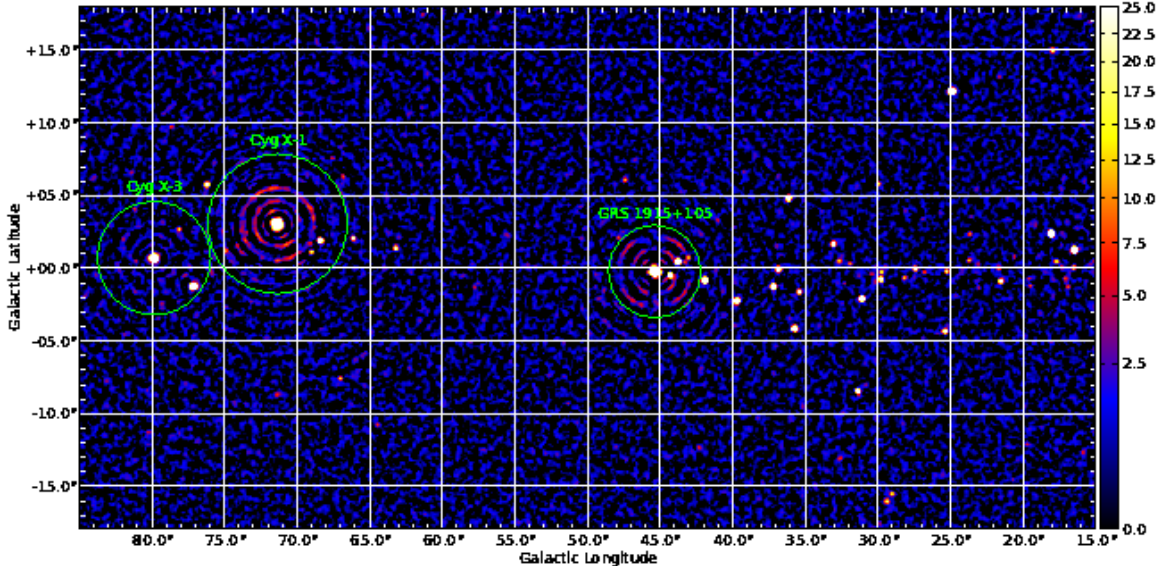


Fig. 3. INTEGRAL/IBIS hard X-ray (17 – 60 keV) map of the sky region of Cyg X-1, Cyg X-3, and GRS 1915+105 at $l = +50^\circ$ with masked area shown as green circles. The corresponding S/N distribution of pixels is shown in Fig. 4.

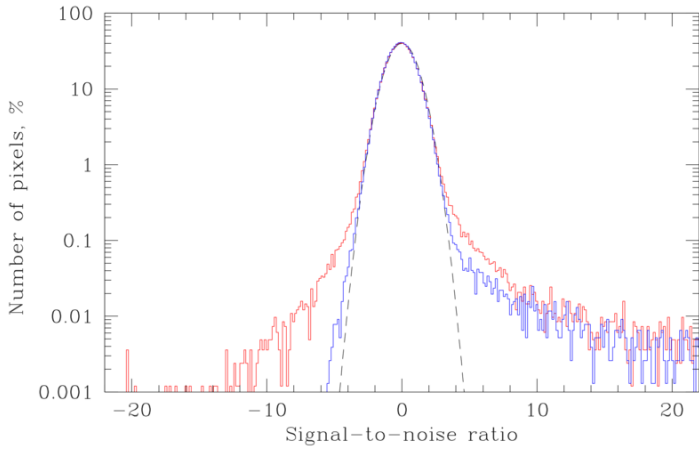


Fig. 4. Signal-to-noise ratio distribution of a number of pixels in the 17 – 60 keV map of Fig. 3. Red and blue histograms show distributions of pixels in full and masked images, respectively. The dashed line represents the normal distribution with unit variance and zero mean.

2.2. Detection threshold

Given the IBIS/ISGRI angular resolution of the survey, the sky map contains $\sim 3 \times 10^5$ statistically independent pixels. Taking into account the minor contribution of the systematic noise, we adopted a conservative detection threshold of $(S/N)_{\text{lim}} > 4.7\sigma$ to ensure that the final catalog contains no more than one spurious source assuming Poisson statistics.

A source detection in the region of ~ 17 degrees around GC should be interpreted with special care because of the possible false peaks induced by the systematic noise. The latter is revealed by a distorted shape that differs significantly from the instrumental point-spread function (PSF), which is a two-dimensional Gaussian ($\sigma = 5'$). The sky map of the GC re-

gion contains 12 peaks above 4.7σ in the reference 17 – 60 keV energy band. All these candidate sources have a very distorted shape, and none of them have been detected in the 35 – 80 keV energy range, which also points to a false detection. Therefore, all excesses in the GC region have been attributed to the systematic noise.

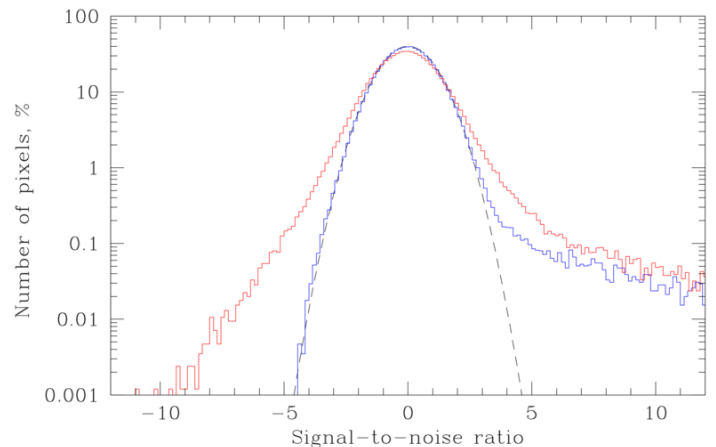


Fig. 6. Signal-to-noise ratio distribution of a number of pixels in the hard X-ray image shown in Fig. 5. The dashed line represents the normal distribution with unit variance and zero mean. Red and blue histograms show pixel distributions for images in the energy band 17 – 60 keV (high systematic noise, see text) and 35 – 80 keV, respectively.

3. Catalog of sources

The catalog was compiled from the source sample exceeding the detection threshold in the reference 17 – 60 keV energy band.

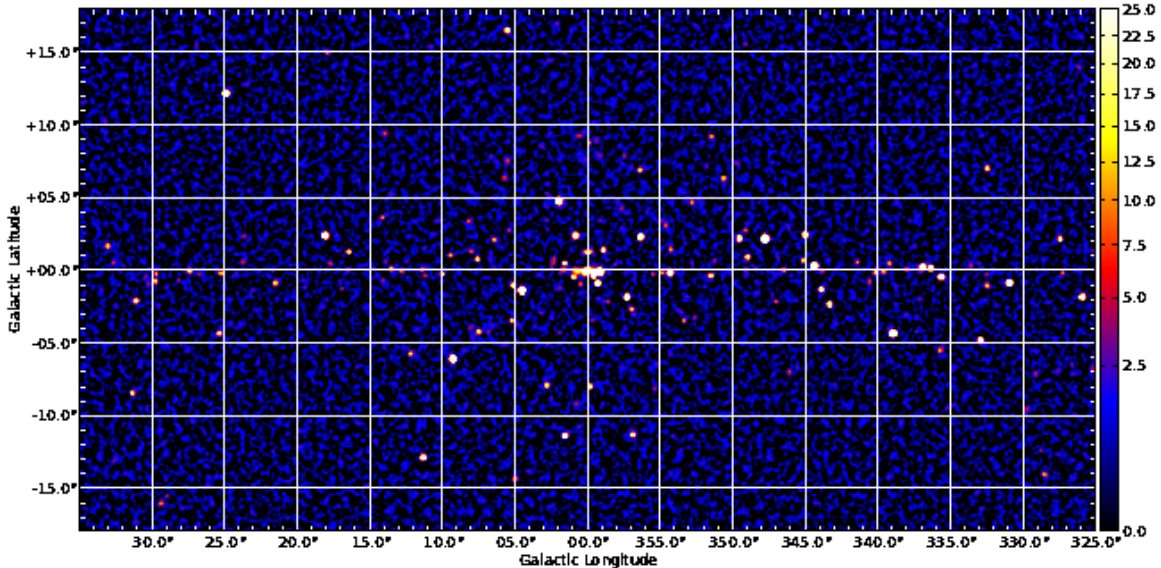


Fig. 5. INTEGRAL/IBIS hard X-ray (35 – 80 keV) map of the sky region around the GC. The total exposure is about 26 Ms in the GC region. The image is shown in terms of S/N with the color map ranging from values of 0 to 25. This color scheme is used to emphasize sky background variations. Fig. 6 demonstrates a corresponding S/N distribution of pixels.

The list of sources is presented in Table 2, and its content is described below.

Column (1) “*Id*” – source sequence number in the catalog.

Column (2) “*Name*” – source name. Their common names are given for sources whose nature was known before their detection by INTEGRAL. Sources discovered by INTEGRAL or those whose nature was established thanks to INTEGRAL observations are named “IGR”

Columns (3,4) “*RA, Dec*” – source equatorial (J2000) coordinates.

Column (5,6,7) “*Flux*” – time-averaged source flux in the 17 – 60 keV, 17 – 35 keV, and 35 – 80 keV energy bands, respectively.

Column (8) “*Type*” – general astrophysical type of the object: LMXB (HMXB) – low- (high-) mass X-ray binary, AGN – active galactic nucleus, SNR – supernova remnant, CV – cataclysmic variable, PSR – isolated pulsar or pulsar wind nebula (PWN), SGR – soft gamma repeater, RS CVn – coronally active binary star, SymbStar – symbiotic star, Cluster – cluster of galaxies. A question mark indicates that the specified type is not firmly determined, so should be confirmed.

Determining of the natures of the sources is complicated and a continually ongoing process. During the compilation of the catalog, we selected from our point of view, the most recent or reliable, identifications from the literature. In some cases (when references are not given), the identifications had been performed using recent observations of the Chandra, XMM-Newton, and Swift observatories, both the Simbad³ and NED⁴ database, as well as the 2MASS catalog.

Column (9) “*Ref*” – references. These are mainly provided for new sources and are related to their discovery and/or nature. The papers describing a routine analysis of a given source e.g.

confirmation of their nature, a refined position, etc. are not referenced.

Column (10) “*Notes*” – additional notes such as type subclass, redshift information, alternative source names. The redshifts of the extragalactic sources were obtained from the Simbad and NED databases.

³ Simbad Astronomical Database <http://simbad.u-strasbg.fr>

⁴ NASA/IPAC Extragalactic Database <http://ned.ipac.caltech.edu>

4. Concluding remarks

Our Galactic survey is based on sky maps averaged over a nine-year time period, which obviously means that it has a strong bias against finding low S/N transient sources. This ensures that the current survey contains mainly persistent objects, in addition to, however, objects with strong intrinsic variability.

We have presented detailed source statistics in Table 3 and a chart of source types in Fig. 7. Our Galactic survey has an identification completeness of $(N_{Tot} - N_{NotID})/N_{Tot} = 1 - 34/402 \approx 0.92$, which provides a strong statistical basis for population studies. In the complementary paper of Lutovinov et al., (2012, in prep.), we note in particular that we used the source sample and sensitivity maps of the current survey to study the HMXB luminosity function and their spatial distribution in the Galactic disk.

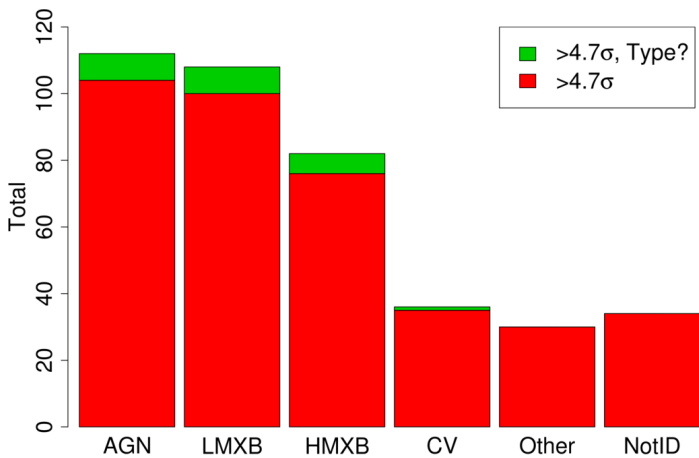


Fig. 7. Chart for the source classes detected at $S/N > 4.7\sigma$ in the reference 17 – 60 keV energy range (see Table 3). Green bar denotes the number of sources that have a tentative association with a given type of objects.

Acknowledgements. The data were obtained from the European and Russian INTEGRAL Science Data Centers^{5,6}. This work was supported by the President of the Russian Federation (through the program supporting leading scientific schools, project NSH-5603.2012.2), by the Presidium of the Russian Academy of Sciences/RAS (program P21 “Non-stationary Phenomena in the Universe”), grants 12-02-01265, 11-02-01328 and 11-02-12285-ofim-2011 from Russian Foundation for Basic Research, State contract 14.740.11.0611. This research has made use of the IGR Sources page⁷ maintained by J. Rodriguez & A. Bodaghee.

References

- Ajello, M., Alexander, D. M., Greiner, J., et al. 2012, arXiv:1202.3137
- Barlow, E. J., Knigge, C., Bird, A. J., J Dean, A., Clark, D. J., Hill, A. B., Molina, M., & Sguera, V. 2006, MNRAS, 372, 224
- Barthelmy, S. D., et al. 2005, Space Science Reviews, 120, 143
- Bassa, C. G., Jonker, P. G., in't Zand, J. J. M., & Verbunt, F. 2006, A&A, 446, L17
- Bassani, L., Malizia, A., Stephen, J. B., et al. 2004, The Astronomer's Telegram, 232, 1
- Bassani, L., et al. 2005, ApJ, 634, L21
- Bassani, L., Molina, M., Malizia, A., et al. 2006, ApJ, 636, L65
- Bassani, L., et al. 2009, MNRAS, 395, L1
- Baumgartner, W. H., Tueller, J., Markwardt, C., & Skinner, G. 2010, Bulletin of the American Astronomical Society, 42, 675
- Beckmann, V., et al. 2005, ApJ, 631, 506
- Beckmann, V., et al. 2009, A&A, 505, 417
- Bikmaev, I. F., Sunyaev, R. A., Revnivtsev, M. G., & Burenin, R. A. 2006a, Astronomy Letters, 32, 221
- Bikmaev, I. F., Revnivtsev, M. G., Burenin, R. A., & Sunyaev, R. A. 2006b, Astronomy Letters, 32, 588
- Bikmaev, I. F., Burenin, R. A., Revnivtsev, M. G., Sazonov, S. Y., Sunyaev, R. A., Pavlinsky, M. N., & Sakhibullin, N. A. 2008, Astronomy Letters, 34, 653
- Bird, A. J., et al. 2006, ApJ, 636, 765
- Bird, A. J., et al. 2007, ApJS, 170, 175
- Bird, A. J., et al. 2010, ApJS, 186, 1
- Bodaghee, A., Walter, R., Zurita Heras, J. A., Bird, A. J., Courvoisier, T. J.-L., Malizia, A., Terrier, R., & Ubertini, P. 2006, A&A, 447, 1027
- Bodaghee A., et al., 2007, A&A, 467, 585
- Bodaghee A., Tomsick J. A., Rodriguez J., James J. B., 2012, ApJ, 744, 108
- Brandt, S., Budtz-Jørgensen, C., & Chenevez, J. 2006a, The Astronomer's Telegram, 778, 1
- Brandt, S., Budtz-Jørgensen, C., Chenevez, J., Lund, N., Oxborow, C. A., & Westergaard, N. J. 2006b, The Astronomer's Telegram, 970, 1
- Brandt, S., Budtz-Jørgensen, C., Gotz, D., Hurley, K., & Frontera, F. 2007, The Astronomer's Telegram, 1054, 1
- Burenin, R., Mescheryakov, A., Revnivtsev, M., Bikmaev, I., & Sunyaev, R. 2006, The Astronomer's Telegram, 880, 1
- Burenin, R., Revnivtsev, M., Mescheryakov, A., Bikmaev, I., Pavlinsky, M., & Sunyaev, R. 2007, The Astronomer's Telegram, 1270, 1
- Burenin, R. A., Mescheryakov, A. V., Revnivtsev, M. G., Sazonov, S. Y., Bikmaev, I. F., Pavlinsky, M. N., & Sunyaev, R. A. 2008, Astronomy Letters, 34, 367
- Butler, S. C., et al. 2009, ApJ, 698, 502
- Bélanger, G., et al. 2006, ApJ, 636, 275
- Chaty, S., Rahoui, F., Foellmi, C., et al. 2008, A&A, 484, 783
- Chelovekov, I. V., & Grebenev, S. A. 2007, Astronomy Letters, 33, 807
- Chernyakova, M., Lutovinov, A., Capitanio, F., Lund, N., & Gehrels, N. 2003, The Astronomer's Telegram, 157, 1
- Chernyakova, M., Courvoisier, T. J.-L., Rodriguez, J., & Lutovinov, A. 2005a, The Astronomer's Telegram, 519, 1
- Chernyakova, M., Lutovinov, A., Rodríguez, J., & Revnivtsev, M. 2005b, MNRAS, 364, 455
- Churazov, E., Sunyaev, R., Revnivtsev, M., et al. 2007, A&A, 467, 529
- Goncalves, T. S., Martin, D. C., Halpern, J. P., Eracleous, M., & Pavlov, G. G. 2008, The Astronomer's Telegram, 1623, 1
- Courvoisier, T. J.-L., Walter, R., Rodriguez, J., Bouchet, L., & Lutovinov, A. A. 2003, IAU Circ., 8063, 3
- Cusumano, G., et al. 2010, A&A, 510, A48
- Curran, P. A., Chaty, S., & Zurita Heras, J. A. 2011a, A&A, 533, A3
- Curran, P. A., Chaty, S., Zurita Heras, J. A., Tomsick, J. A., & Maccarone, T. J. 2011b, MNRAS, 417, L26
- Degenaar, N., Jonker, P. G., Torres, M. A. P., et al. 2010, MNRAS, 404, 1591
- Degenaar, N., Altamirano, D., Wijnands, R., 2012, The Astronomer's Telegram, 4219, 1
- Den Hartog, P. R., Kuiper, L., Hermsen, W., Vink, J., In't Zand, J. J. M., Corbet, R. H. D., & Remillard, R. 2005, The Astronomer's Telegram, 394, 1
- Del Monte, E., Evangelista, Y., Feroci, M., et al. 2008, The Astronomer's Telegram, 1445, 1
- Donato, D., Sambruna, R. M., & Gliozzi, M. 2005, A&A, 433, 1163.
- Eckert, D., Walter, R., Kretschmar, P., et al. 2004, The Astronomer's Telegram, 352, 1
- Fiocchi, M., Bassani, L., Bazzano, A., et al. 2010, ApJ, 720, 987
- Funk, S., Hinton, J. A., Moriguchi, Y., et al. 2007, A&A, 470, 249
- Gehrels, N., et al. 2004, ApJ, 611, 1005
- Gibaud, L., Bazzano, A., Bozzo, E., et al. 2011, The Astronomer's Telegram, 3565, 1
- Grebenev, S. A., Ubertini, P., Chenevez, J., Orr, A., & Sunyaev, R. A. 2004a, The Astronomer's Telegram, 275, 1
- Grebenev, S. A., & Sunyaev, R. A. 2004b, The Astronomer's Telegram, 342, 1
- Grebenev, S. A., Molkov, S. V., & Sunyaev, R. A. 2005a, The Astronomer's Telegram, 444, 1
- Grebenev, S. A., Bird, A. J., Molkov, S. V., Soldi, S., Kretschmar, P., Diehl, R., Budz-Jørgensen, C., & McBreen, B. 2005b, The Astronomer's Telegram, 457, 1
- Grebenev, S. A., Molkov, S. V., & Sunyaev, R. A. 2005c, The Astronomer's Telegram, 467, 1
- Grebenev, S. A., & Sunyaev, R. A. 2007a, Astronomy Letters, 33, 149
- Grebenev, S. A., Molkov, S. V., Revnivtsev, M. G., & Sunyaev, R. A. 2007b, ESA Special Publication, 622, 373
- Gros, A., Goldwurm, A., Cadolle-Bel, M., Goldoni, P., Rodriguez, J., Foschini, L., Del Santo, M., & Blay, P. 2003, A&A, 411, L179
- Gänsicke, B. T., et al. 2005, MNRAS, 361, 141

⁵ <http://isdc.unige.ch>

⁶ <http://hea.iki.rssi.ru/rsdc>

⁷ <http://irfu.cea.fr/Sap/IGR-Sources/>

Table 3. Census of Galactic and extragalactic sources at $|b| < 17.5^\circ$

Energy range, keV	AGN	LMXB	HMXB	CV	Other	NotID	Total
17 – 60	104+8 ^s	100+8 ^s	76+6 ^s	35+1 ^s	30	34	402
17 – 35	89+7 ^s	98+7 ^s	74+6 ^s	35+1 ^s	28	22	367
35 – 80	76+4 ^s	80+5 ^s	66+3 ^s	13	26	7	280

Notes. The number of sources with a tentative classification is denoted with S index. Fig. 7 shows the chart for source classes detected in the 17 – 60 keV energy band.

- Harrison, F. A., Boggs, S., Christensen, F., et al. 2010, Proc. SPIE, 7732,
den Hartog, P. R., Hermsen, W., Kuiper, L. M., in't Zand, J. J. M., Winkler, C.,
& Domingo, A. 2004a, The Astronomer's Telegram, 261, 1
den Hartog, P. R., Kuiper, L. M., Corbet, R. H. D., in't Zand, J. J. M., Hermsen,
W., Vink, J., Remillard, R., & van der Klis, M. 2004b, The Astronomer's
Telegram, 281, 1
Halpern, J. P. 2006, The Astronomer's Telegram, 847, 1
Hannikainen, D. C., Rodriguez, J., & Pottschmidt, K. 2003, IAU Circ., 8088, 4
Heinke, C. O., Tomsick, J. A., Yusef-Zadeh, F., & Grindlay, J. E. 2009, ApJ, 701,
1627
Hiemstra, B., Méndez, M., Done, C., et al. 2011, MNRAS, 411, 137
Kalamkar, M., Homan, J., Altamirano, D., et al. 2011, ApJ, 731, L2
Karasev, D., Tsygankov, S., Lutovinov, A., Churazov, E., & Sunyaev, R. 2007a,
The Astronomer's Telegram, 1245, 1
Karasev, D. I., Lutovinov, A. A., & Grebenev, S. A. 2007b, Astronomy Letters,
33, 159
Karasev, D. I., Lutovinov, A. A., & Burenin, R. A. 2010, MNRAS, 409, L69
Karasev D.I., Lutovinov A.A., Revnivtsev M.G., Krivonos R.A., 2012, Astron.
Letters, 38, N10, in press
Keek, S., Kuiper, L., & Hermsen, W. 2006, The Astronomer's Telegram, 810, 1
Kretschmar, P., Mereghetti, S., Hermsen, W., Ubertini, P., Winkler, C., Brandt,
S., & Diehl, R. 2004, The Astronomer's Telegram, 345, 1
Krivonos, R., Vikhlinin, A., Churazov, E., Lutovinov, A., Molkov, S., & Sunyaev,
R. 2005, ApJ, 625, 89
Krivonos, R., Revnivtsev, M., Churazov, E., Sazonov, S., Grebenev, S., &
Sunyaev, R. 2007a, A&A, 463, 957
Krivonos, R., Revnivtsev, M., Lutovinov, A., Sazonov, S., Churazov, E., &
Sunyaev, R. 2007b, A&A, 475, 775
Krivonos, R., Revnivtsev, M., Tsygankov, S., et al. 2010a, A&A, 519, A107
Krivonos, R., Tsygankov, S., Revnivtsev, M., et al. 2010b, A&A, 523, A61
Krivonos, R., Tsygankov, S., Burenin, R., Revnivtsev, M., & Lutovinov, A. 2011,
The Astronomer's Telegram, 3382, 1
Kuiper, L., Hermsen, W., in't Zand, J., & den Hartog, P. R. 2005, The
Astronomer's Telegram, 662, 1
Kuiper, L., Keek, S., Hermsen, W., Jonker, P. G., & Steeghs, D. 2006a, The
Astronomer's Telegram, 684, 1
Kuiper, L., den Hartog, P. R., & Hermsen, W. 2006b, The Astronomer's
Telegram, 939, 1
Kuiper, L., Jonker, P. G., Torres, M. A. P., Rest, A., & Keek, S. 2008, The
Astronomer's Telegram, 1774, 1
Kuulkers, E., Lutovinov, A., Parmar, A., Capitanio, F., Mowlavi, N., & Hermsen,
W. 2003, The Astronomer's Telegram, 149, 1
Kuulkers, E., et al. 2006, The Astronomer's Telegram, 874, 1
Landi, R., Bassani, L., Malizia, A., Stephen, J. B., Bazzano, A., Fiocchi, M., &
Bird, A. J. 2010, MNRAS, 403, 945
Landi, R., Bassani, L., Masetti, N., Bazzano, A., & Bird, A. J. 2011a, The
Astronomer's Telegram, 3271, 1
Landi, R., Bassani, L., Malizia, J. B., Bazzano, Fiocchi, M., & Bird, A. J., 2011b,
Published in Proceedings of the Workshop "The Extreme and Variable High
Energy Sky" (Chia Laguna (Cagliari) , Italy, September 19-23, 2011), PoS,
009
Landi, R., Bassani, L., Masetti, N., Bazzano, A., Tarana, A., & Bird, A. J. 2012,
The Astronomer's Telegram, 4233, 1
Leyder, J.-C., Walter, R., & Rauw, G. 2008, A&A, 477, L29
Linares, M., Watts, A. L., Wijnands, R., et al. 2009, MNRAS, 392, L11
Lutovinov, A. A., & Revnivtsev, M. G. 2003a, Astronomy Letters, 29, 719
Lutovinov, A., Shaw, S., Foschini, L., & Paul, J. 2003b, The Astronomer's
Telegram, 154, 1
Lutovinov, A., Walter, R., Belanger, G., Lund, N., Grebenev, S., & Winkler, C.
2003c, The Astronomer's Telegram, 155, 1
Lutovinov, A., Cadolle Bel, M., Belanger, G., Goldwurm, A., Budtz-Jorgensen,
C., Mowlavi, N., Paul, J., & Orr, A. 2004a, The Astronomer's Telegram, 328,
1
Lutovinov, A., Rodriguez, J., Budtz-Jorgensen, C., Grebenev, S., & Winkler, C.
2004b, The Astronomer's Telegram, 329, 1
Lutovinov, A., Rodriguez, J., Revnivtsev, M., & Shtykovskiy, P. 2005a, A&A,
433, L41
Lutovinov, A., Revnivtsev, M., Gilfanov, M., Shtykovskiy, P., Molkov, S., &
Sunyaev, R. 2005b, A&A, 444, 821
Lutovinov A., Revnivtsev M., Gilfanov, M., & Sunyaev, R. 2007, ESA Special
Publication, 622, 241
Lutovinov, A., Burenin, R., Sazonov, S., et al. 2010a, The Astronomer's
Telegram, 2759, 1
Lutovinov, A. A., Burenin, R. A., Revnivtsev, M. G., Suleimanov, V. F., &
Tkachenko, A. Y. 2010b, Astronomy Letters, 36, 904
Lutovinov, A. A., Burenin, R. A., Revnivtsev, M. G., & Bikmaev, I. F. 2012,
Astronomy Letters, 38, 1
Malizia, A., et al. 2005, ApJ, 630, L157
Malizia, A., Bassani, L., Sguera, V., et al. 2010, MNRAS, 408, 975
Martí, J., Paredes, J. M., Bloom, J. S., et al. 2004, A&A, 413, 309
Markwardt, C. B., Swank, J. H., & Strohmayer, T. E. 2004, The Astronomer's
Telegram, 353, 1
Markwardt, C. B. 2008, The Astronomer's Telegram, 1686, 1
Masetti, N., Palazzi, E., Bassani, L., Malizia, A., & Stephen, J. B. 2004, A&A,
426, L41
Masetti, N., Bassani, L., Bird, A. J., & Bazzano, A. 2005, The Astronomer's
Telegram, 528, 1
Masetti, N., et al. 2006a, A&A, 449, 1139
Masetti, N., et al. 2006b, A&A, 455, 11
Masetti, N., et al. 2006c, A&A, 459, 21
Masetti, N., Bassani, L., Dean, A. J., Ubertini, P., & Walter, R. 2006d, The
Astronomer's Telegram, 715, 1
Masetti, N., Morelli, L., Palazzi, E., Stephen, J., Bazzano, A., Dean, A. J., Walter,
R., & Minniti, D. 2006e, The Astronomer's Telegram, 783, 1
Masetti, N., et al. 2007a, A&A, 470, 331
Masetti, N., et al. 2007b, The Astronomer's Telegram, 1034, 1
Masetti, N., Rigon, E., Maiorano, E., et al. 2007c, A&A, 464, 277
Masetti, N., et al. 2008, A&A, 482, 113
Masetti, N., et al. 2009, A&A, 495, 121
Masetti, N., Landi, R., Sguera, V., et al. 2010a, A&A, 511, A48
Masetti, N., Parisi, P., Palazzi, E., et al. 2010b, A&A, 519, A96
Masetti, N., Parisi, P., Jiménez-Bailón, E., et al. 2012a, A&A, 538, A123
Masetti, N., et al. 2012b, The Astronomer's Telegram, 4248, 1
McGlynn, T., Scollick, K., & White, N. 1998, New Horizons from Multi-
Wavelength Sky Surveys, 179, 465
Mescheryakov, A., Burenin, R., Sazonov, S., Revnivtsev, M., Bikmaev, I.,
Pavlinsky, M., & Sunyaev, R. 2009, The Astronomer's Telegram, 2132, 1
Milisavljevic, D., Fesen, R. A., Parrent, J. T., & Thorstensen, J. R. 2011, The
Astronomer's Telegram, 3146, 1
Molkov, S., Mowlavi, N., Goldwurm, A., Strong, A., Lund, N., Paul, J., &
Oosterbroek, T. 2003, The Astronomer's Telegram, 176, 1
Molkov, S. V., Cherepashchuk, A. M., Lutovinov, A. A., et al. 2004, Astronomy
Letters, 30, 534
Morelli, L., Masetti, N., Bassani, L., Landi, R., Malizia, A., Bird, A. J., Ubertini,
P., & Galaz, G. 2006, The Astronomer's Telegram, 785, 1
Nespoli, E., Fabregat, J., & Mennickent, R. E. 2008a, The Astronomer's
Telegram, 1396, 1
Nespoli, E., Fabregat, J., & Mennickent, R. E. 2008b, A&A, 486, 911
Nespoli, E., Fabregat, J., & Mennickent, R. E. 2010, A&A, 516, A94
Nucita, A. A., Carpano, S., & Guainazzi, M. 2007, A&A, 474, L1
Nucita, A. A., De Paolis, F., Saxton, R., & Read, A. M. 2012, New A, 17, 589
Parisi, P., Masetti, N., Bassani, L., et al. 2012, The Astronomer's Telegram, 4151,
1
Paizis, A., et al. 2007a, ApJ, 657, L109
Paizis, A., Beckmann, V., Gotz, D., et al. 2007b, The Astronomer's Telegram,
1248, 1
Produit, N., Ballet, J., & Mowlavi, N. 2004, The Astronomer's Telegram, 278, 1

- Ratti, E. M., Bassa, C. G., Torres, M. A. P., et al. 2010, MNRAS, 408, 1866
 Reig, P., & Roche, P. 1999, MNRAS, 306, 100
 Renaud, M., Marandon, V., Gotthelf, E. V., et al. 2010b, ApJ, 716, 663
 Revnivtsev, M., Chernyakova, M., Capitanio, F., Westergaard, N. J., Shoenfelder, V., Gehrels, N., & Winkler, C. 2003a, The Astronomer's Telegram, 132, 1
 Revnivtsev, M. G., Sazonov, S. Y., Gilfanov, M. R., & Sunyaev, R. A. 2003b, Astronomy Letters, 29, 587
 Revnivtsev, M., Tuerler, M., Del Santo, M., Westergaard, N. J., Gehrels, N., & Winkler, C. 2003c, IAU Circ., 8097, 2
 Revnivtsev, M. G., Sazonov, S. Y., Gilfanov M. R., Sunyaev, R. A. 2003d, Astronomy Letters, 29, 587
 Revnivtsev, M. G., et al. 2004a, A&A, 425, L49
 Revnivtsev, M. G., et al. 2004b, Astronomy Letters, 30, 382
 Revnivtsev, M. G., Sazonov, S. Y., Molkov, S. V., Lutovinov, A. A., Churazov, E. M., & Sunyaev, R. A. 2006, Astronomy Letters, 32, 145
 Revnivtsev, M., Lutovinov, A., Churazov, E., Sazonov, S., Gilfanov, M., Grebenev, S., & Sunyaev, R. 2008a, A&A, 491, 209
 Revnivtsev M., Sazonov S., Krivonos R., Ritter H., Sunyaev R., 2008b, A&A, 489, 1121
 Revnivtsev, M. G., et al. 2009, Astronomy Letters, 35, 33
 Reynolds, M. T., Miller, J. M., Maitra, D., et al. 2012, The Astronomer's Telegram, 3951, 1
 Rodriguez, J., et al. 2004, The Astronomer's Telegram, 340, 1
 Sazonov, S., Churazov, E., Revnivtsev, M., Vikhlinin, A., & Sunyaev, R. 2005, A&A, 444, L37
 Sazonov, S., Revnivtsev, M., Krivonos, R., Churazov, E., & Sunyaev, R. 2007, A&A, 462, 57
 Sazonov, S., Revnivtsev, M., Burenin, R., Churazov, E., Sunyaev, R., Forman, W. R., & Murray, S. S. 2008, A&A, 487, 509
 Scaringi S., et al., 2010, MNRAS, 401, 2207
 Sguera, V., et al. 2006, ApJ, 646, 452
 Smith, N., & Hartigan, P. 2006, ApJ, 638, 1045
 Soldi, S., Brandt, S., Garau, A. D., Grebenev, S. A., Kuulkers, E., Palumbo, G. G. C., & Tarana, A. 2005, The Astronomer's Telegram, 456, 1
 Soldi, S., et al. 2006, The Astronomer's Telegram, 885, 1
 Steeghs, D., Knigge, C., Drew, J., Unruh, Y., & Greimel, R. 2008, The Astronomer's Telegram, 1653, 1
 Sunyaev, R., Lutovinov, A., Molcov, S., & Deluit, S. 2003a, The Astronomer's Telegram, 181, 1
 Sunyaev, R. A., Grebenev, S. A., Lutovinov, A. A., Rodriguez, J., Mereghetti, S., Gotz, D., & Courvoisier, T. 2003b, The Astronomer's Telegram, 190, 1
 Takahashi, T., Mitsuda, K., Kelley, R., et al. 2010, Proc. SPIE, 7732,
 Terrier, R., Mattana, F., Djannati-Atai, A., Marandon, V., Renaud, M., & Dubois, F. 2008, American Institute of Physics Conference Series, 1085, 312
 Tomsick, J. A., Lingenfelter, R., Walter, R., Rodriguez, J., Goldwurm, A., Corbel, S., & Kaaret, P. 2003, IAU Circ., 8076, 1
 Tomsick, J. A., Lingenfelter, R., Corbel, S., Goldwurm, A., & Kaaret, P. 2004, The Astronomer's Telegram, 224, 1
 Tomsick, J. A., Chaty, S., Rodriguez, J., Foschini, L., Walter, R., & Kaaret, P. 2006, ApJ, 647, 1309
 Tomsick, J. A., Chaty, S., Rodriguez, J., Walter, R., & Kaaret, P. 2008, ApJ, 685, 1143
 Tomsick, J. A., Chaty, S., Rodriguez, J., Walter, R., & Kaaret, P. 2009, ApJ, 701, 811
 Torrejón, J. M., Negueruela, I., Smith, D. M., & Harrison, T. E. 2010, A&A, 510, A61
 Torres, M. A. P., Garcia, M. R., McClintock, J. E., et al. 2004, The Astronomer's Telegram, 264, 1
 Torres, M. A. P., Steeghs, D., Garcia, M. R., et al. 2006, The Astronomer's Telegram, 862, 1
 Torres, M. A. P., Steeghs, D., Jonker, P. G., Garcia, M. R., Challis, P., Modjaz, M., & Kirshner, R. P. 2007, The Astronomer's Telegram, 1286, 1
 Tueller, J., Baumgartner, W. H., Markwardt, C. B., et al. 2010, ApJS, 186, 378
 Tuerler, M., Walter, R., & Ferrigno, C. 2012, The Astronomer's Telegram, 4183, 1
 Ubertini P., et al., 2003, A&A, 411, L131
 Ubertini, P., et al. 2005, ApJ, 629, L109
 Walter, R., et al. 2004, The Astronomer's Telegram, 229, 1
 Walter, R., et al. 2006, A&A, 453, 133
 Watson, M. G., et al. 2009, A&A, 493, 339
 Wijnands, R. 2006, The Astronomer's Telegram, 972, 1
 Winkler C., et al., 2003, A&A, 411, L1
 Winter, L. M., Mushotzky, R. F., Tueller, J., & Markwardt, C. 2008, ApJ, 674, 686
 Zurita Heras, J. A., Chaty, S., & Tomsick, J. A. 2009, A&A, 502, 787
 in't Zand, J. J. M. 2005, A&A, 441, L1
 Zolotukhin, I. Y., & Revnivtsev, M. G. 2011, MNRAS, 411, 620

Table 2. The catalog of sources[†] detected during the INTEGRAL/IBIS nine-year Galactic survey.

Id	Name	RA deg	Dec deg	F _{17–60 keV} [*] erg cm ⁻² s ⁻¹		F _{17–35 keV} [*] erg cm ⁻² s ⁻¹		F _{35–80 keV} [*] erg cm ⁻² s ⁻¹		Type	Ref.*	Notes**
				erg cm ⁻² s ⁻¹	erg cm ⁻² s ⁻¹	erg cm ⁻² s ⁻¹	erg cm ⁻² s ⁻¹	erg cm ⁻² s ⁻¹	erg cm ⁻² s ⁻¹			
1	IGR J00040+7020	1.009	70.326	0.85 ± 0.12 (7.4)	0.50 ± 0.08 (6.5)	0.39 ± 0.12 (3.3)				AGN	1	Sy2 z=0.096;
2	IGR J00234+6141	5.740	61.684	0.73 ± 0.09 (8.5)	0.55 ± 0.06 (9.6)	< 0.18				CV	2,3	
3	TYCHO SNR	6.332	64.140	0.88 ± 0.09	0.56 ± 0.06 (9.7)	0.46 ± 0.09 (5.0)				SNR		Sy2 z=0.012; ↴
4	SWIFT J0025.8+6818	6.374	68.357	0.83 ± 0.10 (8.2)	0.45 ± 0.07 (6.6)	0.69 ± 0.11 (6.6)				AGN		↪ =IGR J00255+6821442;
5	V709 Cas	7.204	59.292	5.10 ± 0.09	3.31 ± 0.06	2.16 ± 0.10				CV	4	V* V1037 Cas
6	IGR J00291+5934	7.263	59.572	2.33 ± 0.09	1.27 ± 0.06	1.58 ± 0.09				LMXB	5,6	Sy1.5 z=0.105; ↴
7	IGR J00335+6126	8.331	61.463	0.61 ± 0.09 (7.0)	0.37 ± 0.06 (6.2)	0.37 ± 0.09 (4.0)				AGN	7,8	↪ =IGR J00333+6122;
8	87GB00330.9+593328	8.973	59.828	1.17 ± 0.09	0.82 ± 0.06	0.45 ± 0.10 (4.7)				HMXB	9	Blazar z=0.086;
9	IGR J00370+6122	9.286	61.382	0.80 ± 0.09 (9.1)	0.43 ± 0.06 (7.2)	0.53 ± 0.09 (5.7)				Star	10	
10	Gamma Cas	14.179	60.715	4.88 ± 0.10	3.72 ± 0.06	1.20 ± 0.10						
11	1A 0114+650	19.514	65.289	10.99 ± 0.10	7.35 ± 0.07	4.56 ± 0.11						
12	4U0115+63	19.630	63.743	37.69 ± 0.10	27.99 ± 0.07	9.77 ± 0.11						
13	4U0142+61	26.594	61.751	2.63 ± 0.12	1.02 ± 0.08	2.88 ± 0.13						
14	RJ0146.9+6121	26.674	61.360	1.32 ± 0.12	0.73 ± 0.08 (8.8)	0.55 ± 0.13 (4.3)						Sy2 z=0.034; LEDA 166414?
15	IGR J01545+6437	28.688	64.624	0.65 ± 0.13 (5.1)	0.36 ± 0.09 (4.2)	0.36 ± 0.13 (2.7)						Sy1 z=0.0492; LEDA 138501; ↴
16	IGR J02095+5226	32.411	52.447	2.94 ± 0.25	1.84 ± 0.17	1.61 ± 0.26 (6.2)						↪ IES 0206+522;
17	IGR J02164+5126	34.103	51.441	1.73 ± 0.28 (6.3)	0.93 ± 0.19 (5.0)	0.78 ± 0.29 (2.7)				AGN	8,14	Sy2 z=0.422;
18	QSO B0212+73	34.419	73.839	1.91 ± 0.25 (7.5)	0.97 ± 0.17 (5.7)	1.54 ± 0.26 (5.8)				AGN		Quasar z=2.367; ↴
19	LSI +61 303	40.114	61.210	1.96 ± 0.18	1.05 ± 0.12 (8.8)	1.45 ± 0.18 (7.9)				HMXB		↪ SWIFT J0218.0+7348;
20	4U 0241+61	41.233	62.463	4.03 ± 0.18	2.10 ± 0.12	3.07 ± 0.19				AGN		IGR J02403+6113; V* V615 Cas
21	SWIFT J0250.2+4650	42.608	46.792	1.48 ± 0.27 (5.4)	0.86 ± 0.19 (4.6)	< 0.55				AGN	15,16	Sy1 z=0.044557; ↴
22	IGR J02501+5440	42.644	54.720	1.15 ± 0.24 (4.9)	0.85 ± 0.16 (5.3)	0.68 ± 0.24 (2.8)				AGN	7,1	↪ 2MASX J02502722+4647295;
23	PERSEUS CLUSTER	49.982	41.515	3.55 ± 0.19	2.78 ± 0.13	1.16 ± 0.21 (5.4)				Cluster	17,18	Sy2 z=0.015; ↴
24	IGR J03249+4041	51.272	40.713	0.98 ± 0.19 (5.2)	0.52 ± 0.13 (4.2)	0.87 ± 0.21 (4.2)				AGN		↪ IGR J02504+5443 (LEDA 166445); Thermal emission dominates; Sy2 z=0.0476; interacting galaxies ↴
25	GK Per	52.798	43.882	2.44 ± 0.20	1.55 ± 0.13	0.97 ± 0.21 (4.5)				CV	19,20	↪ LEDA 097012;
26	IGR J03334+3718	53.355	37.304	1.51 ± 0.17 (8.7)	0.74 ± 0.12 (6.3)	0.92 ± 0.19 (4.7)				AGN		↪ 2MASX J03251221+404021;
27	V0332+53	53.751	53.173	165.13 ± 0.25	109.49 ± 0.17	30.19 ± 0.25				HMXB		=PBC J0325.1+4042;
28	4U 0352+30	58.846	31.041	42.41 ± 0.19	23.38 ± 0.13	28.46 ± 0.21				HMXB		↪ RX J0325.2+4042;
29	IGR J04059+5416	61.499	54.276	1.23 ± 0.25 (4.9)	0.85 ± 0.17 (4.9)	0.60 ± 0.25 (2.4)				AGN		↪ SWIFT J0324.9+4044;
30	3C11	64.582	38.025	5.99 ± 0.20	3.16 ± 0.13	4.30 ± 0.22				AGN	21,22	Sy1 z=0.0485;
31	IGR J04221+4856	65.527	48.948	1.03 ± 0.19 (5.3)	0.66 ± 0.13 (5.0)	0.69 ± 0.21 (3.3)				AGN		Sy1 z=0.114; ↴
32	RX J0440.9+4431	70.241	44.532	5.74 ± 0.18	3.51 ± 0.12	3.03 ± 0.20				HMXB	23	↪ 1RXS J042201.0+485610;
33	UGC03142	70.982	28.993	2.56 ± 0.24	1.37 ± 0.16 (8.3)	1.92 ± 0.25 (7.7)				AGN		Sy1 z=0.021828; ↴
												↪ 1RXS J044350.8+285845;

Table 2. Continued.

Id	Name	RA [†] deg	Dec [‡] deg	F _{17–60 keV} [*] erg cm ⁻² s ⁻¹	F _{7–35 keV} [*] erg cm ⁻² s ⁻¹	F _{35–80 keV} [*] erg cm ⁻² s ⁻¹	Type	Ref. ^{**}	Notes ^{***}
34	LEDA 168563	73.034	49.550	2.57 ± 0.19	1.41 ± 0.13	1.62 ± 0.21 (7.6)	AGN	12	Sy1 z=0.029; ↓ ↓ =IRXS J045205.0+493248; non-magnetic CV; ↓ ↓ =IRXS J045707.4+452751;
35	IGR J04571+4527	74.302	45.468	1.32 ± 0.19 (7.1)	1.03 ± 0.12 (8.3)	< 0.41	CV		
36	V1062 Tau	75.617	24.776	0.90 ± 0.18 (5.0)	0.68 ± 0.13 (5.4)	0.60 ± 0.18 (3.3)	CV		
37	IGR J05081+1722	77.036	17.345	1.53 ± 0.18 (8.6)	0.67 ± 0.12 (5.4)	1.19 ± 0.18 (6.5)	AGN		Sy2 z=0.0177; ↓ ↓ =2MASX J05081967+1721483; Sy1 z=0.017879;
38	IRAS 05078+1626	77.685	16.499	5.39 ± 0.18	3.04 ± 0.12	3.08 ± 0.18	AGN	24	Quasar z=2.07; ↓ ↓ high systematic noise from Crab;
39	RX J0525.3+2413	81.390	24.223	0.86 ± 0.15 (5.9)	0.59 ± 0.10 (5.7)	< 0.29	CV		
40	PKS 0528+134	82.774	13.573	1.17 ± 0.17 (6.8)	0.58 ± 0.12 (4.9)	0.74 ± 0.18 (4.1)	AGN		
41	Crab	83.630	22.016	1360.35 ± 0.14	788.72 ± 0.10	830.54 ± 0.14	PSR		
42	A 0535+262	84.730	26.316	87.32 ± 0.15	44.86 ± 0.10	96.24 ± 0.15	HMXB		
43	BY Cam	85.718	60.852	2.34 ± 0.39 (6.0)	1.53 ± 0.26 (5.9)	1.05 ± 0.42 (2.5)	CV	4	Sy2 z=0.036; ↓ ↓ =2MASX J05471492+5038251;
44	IGR J05470+5034	86.817	50.604	1.28 ± 0.27 (4.8)	0.73 ± 0.18 (4.1)	0.79 ± 0.30 (2.7)	AGN	16	Sy2 z=0.007579; Sy1 z=0.020484; V* V405 Aur; DQ Her type Sy1 z=0.033; ↓ ↓ =SWIFT J0602.2+2829;
45	NGC 2110	88.047	-7.462	14.87 ± 0.25	7.89 ± 0.17	10.75 ± 0.26	AGN		
46	MCG 8-11-11	88.727	46.435	10.72 ± 0.28	6.05 ± 0.19	6.55 ± 0.31	AGN		
47	SWIFT J0558.0+5352	89.531	53.912	2.22 ± 0.33 (6.7)	1.32 ± 0.22 (6.0)	0.87 ± 0.36 (2.4)	CV		
48	IRAS 05589+2828	90.551	28.467	3.23 ± 0.17	1.74 ± 0.12	2.11 ± 0.17	AGN		
49	4U 0614+091	94.282	9.136	25.51 ± 0.31	16.00 ± 0.21	12.61 ± 0.33	LMXB	25	Sy2 z=0.017195; ↓ ↓ =SWIFT J0641.3+3257;
50	IGR J06415+3251	100.368	32.861	3.11 ± 0.36 (8.7)	1.93 ± 0.24 (8.0)	1.54 ± 0.38 (4.0)	AGN		
51	MXB 0656-072	104.573	-7.209	3.83 ± 0.20	2.52 ± 0.14	1.10 ± 0.21 (5.3)	HMXB		
52	SWIFT J0732.5-1331	113.147	-13.512	2.12 ± 0.20	1.37 ± 0.14 (9.7)	1.10 ± 0.21 (5.3)	CV		
53	IGR J07563-4137	119.071	-41.645	1.05 ± 0.14 (7.4)	0.56 ± 0.10 (5.7)	0.77 ± 0.14 (5.3)	AGN	26,27	DQ Her type ↓ =IGR J07565-4139; Sy2 z=0.021; ↓ ↓ =IGR J07565-4139;
54	IGR J07597-3842	119.930	-38.719	2.85 ± 0.16	1.49 ± 0.11	1.83 ± 0.16	AGN		
55	ESO 209-G012	120.490	-49.759	1.65 ± 0.13	0.91 ± 0.09	1.10 ± 0.13 (8.3)	AGN		
56	IGR J08297-4250	127.450	-42.848	0.50 ± 0.10 (5.0)	0.28 ± 0.07 (4.1)	0.36 ± 0.10 (3.5)	PSR		
57	Vela pulsar	128.834	-45.181	8.97 ± 0.09	4.95 ± 0.06	5.98 ± 0.10	LMXB		
58	4U 0836-429	129.349	-42.897	15.83 ± 0.10	9.01 ± 0.07	9.50 ± 0.10	AGN		
59	FAIRALL 1146	129.629	-35.990	1.67 ± 0.14	1.04 ± 0.10	0.86 ± 0.15 (5.8)	AGN		
60	IGR J08390-4833	129.699	-48.524	0.84 ± 0.10 (8.7)	0.48 ± 0.07 (7.3)	0.29 ± 0.10 (2.9)	CV	28,29	Sy1 z=0.039587; Sy1 z=0.04;
61	Vela X-1	135.531	-40.556	256.94 ± 0.11	186.29 ± 0.08	68.98 ± 0.11	HMXB		
62	IGR J09026-4812	135.652	-48.230	1.58 ± 0.10	0.86 ± 0.07	1.05 ± 0.10	AGN	32	Sy1 z=0.0391;
63	IRAS 09149-6206	139.041	-62.340	2.04 ± 0.18	1.14 ± 0.12 (9.3)	1.10 ± 0.19 (5.9)	LMXB		Sy1 z=0.05715;
64	IGR J09189-4418	139.730	-44.305	0.51 ± 0.11 (4.7)	0.23 ± 0.07 (3.2)	0.38 ± 0.11 (3.4)	AGN		Sy2 z=0.008226; ↓ ↓ =ESO 434-C040;
65	X 0918-548	140.105	-55.205	4.48 ± 0.13	2.86 ± 0.09	2.44 ± 0.13	HMXB		Sy1 z=0.252; ↓ ↓ =IGR J09523-6231;
66	MCG-5-23-16	146.922	-30.947	11.84 ± 0.35	6.64 ± 0.24	7.45 ± 0.37	AGN		ESO 263-G013; ↓ ↓ =Sy2 z=0.032859;
67	IGR J09522-6231	148.097	-62.545	0.99 ± 0.14 (6.9)	0.54 ± 0.10 (5.6)	0.77 ± 0.15 (5.3)	AGN	30	
68	SWIFT J0958.0-4208	149.419	-42.126	1.35 ± 0.19 (7.0)	0.92 ± 0.13 (7.0)	0.69 ± 0.20 (3.4)			
69	GRO J1008-57	152.450	-58.292	4.94 ± 0.12	3.19 ± 0.08	2.05 ± 0.12			
70	IGR J10095-4248	152.454	-42.810	2.17 ± 0.23 (9.4)	1.06 ± 0.16 (6.7)	1.55 ± 0.24 (6.5)			

Table 2. Continued.

Id	Name	RA [†] deg	Dec [‡] deg	F _{17–60 keV} [*] erg cm ⁻² s ⁻¹	F _{17–35 keV} [*] erg cm ⁻² s ⁻¹	F _{35–80 keV} [*] erg cm ⁻² s ⁻¹	Type	Ref. ^{**}	Notes ^{***}
71	IGR J10100-5655	152.529	-56.912	1.02 ± 0.12 (8.3)	0.66 ± 0.08 (7.8)	0.47 ± 0.13 (3.7)	HMXB CV	33,29 34,35	IGR J10101-5654 RXP J10103-0-574810; ↴ ↳ Symbiotic binary;
72	IGR J10109-5746	152.778	-57.802	1.51 ± 0.12	1.00 ± 0.08	0.62 ± 0.12 (5.0)	HMXB AGN	36	Sy1 z=0.060; ↴ ↳ SWIFT J1038.8-4942;
73	3U 1022-55	159.415	-56.794	1.07 ± 0.12 (9.2)	0.75 ± 0.08 (9.4)	0.31 ± 0.12 (2.7)	HMXB AGN	26,37 38,39	LEDA 93974; Sy2 z=0.024027; 2MASS J10445192-6025115;
74	IGR J10386-4947	159.688	-49.782	1.24 ± 0.17 (7.5)	0.49 ± 0.11 (4.3)	0.85 ± 0.17 (5.0)	Star	40	WRAY 15-793; 2E 1118.7-6138; ↳ SWIFT J1120.9-6155;
75	IGR J10404-4625	160.140	-46.397	1.77 ± 0.24 (7.5)	0.82 ± 0.16 (5.1)	1.67 ± 0.24 (7.0)	AGN	36	
76	IGR J10447-6027	161.162	-60.437	0.74 ± 0.11 (6.6)	0.38 ± 0.08 (4.9)	0.47 ± 0.11 (4.2)			
77	ETA CAR	161.240	-59.714	0.66 ± 0.11 (5.9)	0.28 ± 0.08 (3.6)	0.50 ± 0.11 (4.4)			
78	IGR J11187-5438	169.594	-54.662	0.65 ± 0.12 (5.3)	0.33 ± 0.09 (3.9)	0.41 ± 0.12 (3.3)			
79	1A 1118-61	170.231	-61.922	4.75 ± 0.11	2.90 ± 0.08	1.90 ± 0.11	HMXB		
80	Cen X-3	170.311	-60.625	64.71 ± 0.11	54.09 ± 0.08	7.84 ± 0.11	HMXB		
81	IGR J11305-6256	172.773	-62.950	2.85 ± 0.11	1.94 ± 0.08	0.94 ± 0.11 (8.2)	HMXB AGN	41,42 1	LINER Sy2 z=0.014; ↴ ↳ =IGR J11366-6002;
82	IGR J11361-6003	174.082	-60.067	0.80 ± 0.11 (7.2)	0.46 ± 0.08 (5.9)	0.43 ± 0.11 (3.8)			
83	IGR J11435-6109	175.994	-61.128	3.67 ± 0.11	2.20 ± 0.08	1.96 ± 0.11	HMXB	43,8	Sy 1,2, z=0.244; ↴ ↳ 2MASS J11453362-6954017;
84	IGR J11459-6955	176.526	-69.943	0.97 ± 0.17 (5.7)	0.41 ± 0.12 (3.5)	0.66 ± 0.17 (3.9)	AGN	12	C86; C85;
85	A1145.1-6141	176.863	-61.971	23.91 ± 0.11	15.47 ± 0.08	10.75 ± 0.11	HMXB		
86	X1145-619	177.000	-62.207	2.43 ± 0.11	1.47 ± 0.08	1.13 ± 0.11 (9.9)	HMXB AGN	34,27	WKK0560; Sy2 z=0.028368;
87	IGR J12026-5349	180.690	-53.837	2.92 ± 0.15	1.60 ± 0.10	1.71 ± 0.15	HMXB	44	4U 1210-64
88	IES 1210-646	183.266	-64.879	1.15 ± 0.12 (9.4)	0.83 ± 0.09 (9.7)	0.36 ± 0.12 (2.9)	AGN?	45	IRXS J121324.5-601458;
89	IGR J12134-6015	183.366	-60.251	0.63 ± 0.12 (5.4)	0.28 ± 0.08 (3.4)	0.56 ± 0.11 (5.0)			
90	GX 301-2	186.654	-62.772	220.81 ± 0.12	174.28 ± 0.08	29.58 ± 0.12	HMXB CV	46	V* RT Cru; Sy1,5 z=0.024; ↴
91	XSS J12270-4859	186.990	-48.887	1.82 ± 0.21 (8.7)	0.95 ± 0.14 (6.6)	1.21 ± 0.21 (5.6)	SymbStr AGN	47,48	Sy1,5 z=0.028; ↴ ↳ =IGR J1241.5-5750;
92	IGR J12349-6434	188.730	-64.564	4.53 ± 0.12	2.79 ± 0.08	2.13 ± 0.12			
93	WKK 1263	190.372	-57.828	1.70 ± 0.13	0.88 ± 0.09	0.99 ± 0.13 (7.8)			
94	IGR J12480-5829	192.013	-58.458	0.70 ± 0.12 (5.7)	0.27 ± 0.09 (3.2)	0.65 ± 0.12 (5.2)	AGN	11,12	
95	4U 1246-588	192.405	-59.095	4.09 ± 0.12	2.53 ± 0.08	2.29 ± 0.12	LMXB	49	
96	2S1254-690	194.416	-69.283	2.76 ± 0.14	2.46 ± 0.10	< 0.29	LMXB		
97	4U 1258-61	195.316	-61.601	2.15 ± 0.12	1.30 ± 0.08	0.95 ± 0.12 (8.1)	HMXB	50	V* V850 Cen
98	IRXP J130.159.6-635806	195.495	-63.969	2.17 ± 0.12	1.48 ± 0.08	1.08 ± 0.12 (9.1)	HMXB	50	C99;
99	PSR B1259-63	195.699	-63.836	1.35 ± 0.12	0.81 ± 0.08 (9.9)	1.00 ± 0.12 (8.4)	HMXB	50	C98;
100	NGC 4945	196.365	-49.469	15.62 ± 0.17	7.38 ± 0.11	13.03 ± 0.17	AGN	34,1	Sy2 z=0.001908; IGR J13109-5552; Sy1 z=0.104;
101	IGR J13107-5551	197.696	-55.874	1.64 ± 0.13	0.79 ± 0.09 (8.8)	1.22 ± 0.13 (9.2)	AGN		
102	IGR J131.86-6257	199.621	-62.958	0.99 ± 0.11 (8.6)	0.68 ± 0.08 (8.6)	0.48 ± 0.12 (4.2)	HMXB?	51	
103	4U 1323-619	201.651	-62.134	11.49 ± 0.11	7.04 ± 0.08	5.90 ± 0.12	LMXB AGN		
104	4U 1344-60	206.899	-60.618	5.49 ± 0.11	3.04 ± 0.08	3.46 ± 0.12 (6.3)	PWN	52,53	Sy1.5 z=0.013; ms pulsar
105	IGR J14003-6326	210.128	-63.419	1.14 ± 0.12 (9.2)	0.73 ± 0.08 (9.2)	0.75 ± 0.12 (6.3)			
106	IGR J14091-6108	212.274	-61.142	0.60 ± 0.11 (5.2)	0.47 ± 0.08 (5.9)	< 0.24			
107	Circinus galaxy	213.292	-65.341	16.85 ± 0.12	9.43 ± 0.08	9.93 ± 0.12	AGN		Sy2 z=0.001421;
108	IGR J14175-4641	214.267	-46.684	1.31 ± 0.14 (9.1)	0.67 ± 0.10 (6.9)	0.81 ± 0.15 (5.3)	AGN	34,29	Sy2 z=0.076;
109	4U 1416-62	215.284	-62.681	1.04 ± 0.12 (9.0)	0.65 ± 0.08 (8.2)	0.48 ± 0.12 (4.0)	HMXB		

Table 2. Continued.

Id	Name	RA [†] deg	Dec [‡] deg	F _{17–60 keV} [*] erg cm ⁻² s ⁻¹	F _{17–35 keV} [*] erg cm ⁻² s ⁻¹	F _{35–80 keV} [*] erg cm ⁻² s ⁻¹	Type	Ref. ^{**}	Notes ^{***}
110	IGR J14257-6117	216.413	-61.306	0.73 ± 0.12 (6.3)	0.41 ± 0.08 (5.1)	0.45 ± 0.12 (3.7)	LMXB	52,1	Swift J1424.8-6122;
111	IGR J14298-6715	217.457	-67.237	1.04 ± 0.13 (8.0)	0.58 ± 0.09 (6.5)	0.45 ± 0.13 (3.4)	AGN	52,1	IRXS J142959.9-671447
112	NGC 5643	218.169	-44.189	1.02 ± 0.14 (7.3)	0.50 ± 0.09 (5.4)	0.76 ± 0.15 (5.2)	HMXB	52,1	Sy2 z=0.003943;
113	IGR J14331-6112	218.264	-61.266	0.90 ± 0.12 (7.8)	0.63 ± 0.08 (8.0)	0.35 ± 0.12 (2.9)	AGN	52,1	Sy1,2 z=0.053;
114	IGR J14471-6414	221.603	-64.275	0.99 ± 0.12 (8.1)	0.39 ± 0.08 (4.6)	0.97 ± 0.13 (7.6)	AGN	34,29	Sy2 z=0.038;
115	IGR J14471-6319	221.806	-63.285	0.75 ± 0.12 (6.2)	0.36 ± 0.08 (4.4)	0.65 ± 0.12 (5.2)	AGN	54	Sy2 (?) ; IGR J14488-4008
116	IGR J14488-4009	222.199	-40.148	0.71 ± 0.13 (5.4)	0.47 ± 0.09 (5.4)	0.30 ± 0.14 (2.2)	AGN?	30	2MASX J14491283-5516194;
117	IGR J14493-5534	222.322	-55.596	1.41 ± 0.12	0.76 ± 0.08 (9.2)	0.92 ± 0.12 (7.4)	AGN	33,29	WKK 4374; Sy2 z=0.018;
118	IGR J14515-5542	222.900	-55.684	1.48 ± 0.12	0.80 ± 0.08 (9.8)	1.08 ± 0.12 (8.7)	AGN	33,46	Polar
119	IGR J14536-5522	223.403	-55.354	1.02 ± 0.12 (8.5)	0.77 ± 0.08 (9.4)	0.34 ± 0.12 (2.8)	CV	34,29	WKK 4438; Sy1 z=0.016;
120	IGR J14552-5133	223.836	-51.577	1.07 ± 0.13 (8.5)	0.60 ± 0.09 (7.1)	0.67 ± 0.13 (5.2)	AGN	34,29	Sy2 z=0.016261;
121	IC 4518A	224.421	-43.130	1.75 ± 0.13	0.97 ± 0.09	0.86 ± 0.13 (6.3)	AGN	55	PMN J1508-4953; ↴
122	SWIFT J1508.6-4953	227.154	-49.874	0.75 ± 0.12 (6.3)	0.43 ± 0.08 (5.3)	0.65 ± 0.12 (5.4)	AGN	34,46	↳ Radio-source;
123	IGR J15094-6649	227.341	-66.828	1.79 ± 0.14	1.16 ± 0.10	0.58 ± 0.15 (4.0)	CV	34,56	=IGR J15359-5750; ↴
124	PSR 1509-58	228.483	-59.143	10.94 ± 0.12	5.73 ± 0.08	7.93 ± 0.12	PSR	57	↳ CXO J153602.7-574853;
125	4U 1516-569	230.169	-57.168	5.84 ± 0.12	5.16 ± 0.08	0.39 ± 0.12 (3.4)	LMXB	51	SWIFT J1539.2-6227
126	IGR J15335-5420	233.373	-54.358	0.55 ± 0.11 (5.1)	0.33 ± 0.07 (4.4)	0.42 ± 0.11 (3.9)	AGN?	34,56	Galactic source; ↴
127	IGR J15360-5750	234.002	-57.814	1.44 ± 0.12	0.78 ± 0.08 (9.9)	0.94 ± 0.12 (8.1)	AGN?	34,56	↳ =IGR J15415-5029;
128	IGR J15390-6226	234.793	-62.474	1.00 ± 0.13 (7.5)	0.53 ± 0.09 (5.9)	0.52 ± 0.14 (3.8)	LMXB?	57	
129	IGR J15414-5030	235.389	-50.491	0.63 ± 0.10 (6.1)	0.39 ± 0.07 (5.4)	0.39 ± 0.10 (3.8)	CV?	51	
130	4U 1538-522	235.597	-52.386	21.58 ± 0.10	16.61 ± 0.07	4.73 ± 0.10	LMXB	52,58	
131	XTE J1543-568	236.024	-56.729	0.55 ± 0.11 (4.9)	0.17 ± 0.08 (2.2)	0.37 ± 0.11 (3.3)	HMXB	12	ESO 136-6; Sy2 z=0.014997;
132	4U 1543-624	236.963	-62.571	3.22 ± 0.14	2.64 ± 0.09	0.42 ± 0.14 (3.0)	LMXB	12	↳ two AGNs ² ;
133	NY Lup	237.057	-45.477	5.99 ± 0.11	3.72 ± 0.07	2.99 ± 0.11	CV	12	Sy1 z=0.016; ↴
134	1E 1547.0-5408	237.729	-54.295	1.52 ± 0.10	0.65 ± 0.07 (9.1)	1.39 ± 0.10	PSR	12	WKK 6471; Sy1 z=0.035;
135	XTE J1550-564	237.746	-56.475	19.41 ± 0.11	9.32 ± 0.08	15.98 ± 0.11	LMXB	12	AX J161929-4945;
136	IGR J15539-6142	238.423	-61.679	0.88 ± 0.14 (6.5)	0.33 ± 0.09 (3.6)	0.77 ± 0.14 (5.6)	AGN	12	SyXB; IRXS J161933.6-280736; ↴
137	ESO 389-G 002	238.712	-37.661	0.89 ± 0.15 (6.0)	0.62 ± 0.10 (6.1)	0.48 ± 0.15 (3.2)	LMXB	12	↳ =IGR J16119-6036; ↴
138	4U 1556-605	240.303	-60.704	0.80 ± 0.13 (6.0)	0.57 ± 0.09 (6.3)	<0.27	AGN	59	SWIFT J1605.7-7250; ↴
139	IGR J16058-7253	241.481	-72.901	1.59 ± 0.22 (7.3)	0.86 ± 0.15 (5.9)	1.00 ± 0.23 (4.3)	AGN	59	
140	WKK 6092	242.998	-60.631	1.49 ± 0.13	0.85 ± 0.09 (9.2)	1.09 ± 0.14 (8.0)	AGN	59	
141	4U 1608-522	243.179	-52.424	24.14 ± 0.10	15.22 ± 0.07	12.39 ± 0.10	LMXB	60,4	
142	IGR J16167-4957	244.141	-49.978	1.67 ± 0.09	1.18 ± 0.07	0.40 ± 0.09 (4.3)	CV	60,4	IRXS J161637.2-495847;
143	IGR J16175-5059	244.350	-50.937	0.62 ± 0.09 (6.5)	0.30 ± 0.07 (4.5)	0.64 ± 0.09 (6.8)	PSR	60,4	PSR J1617-5055
144	IGR J16181-5407	244.525	-54.113	0.53 ± 0.10 (5.3)	0.32 ± 0.07 (4.6)	0.24 ± 0.10 (2.4)	2PBC J1618.1-5405	60,4	
145	IGR J16185-5928	244.648	-59.465	1.20 ± 0.13 (9.4)	0.63 ± 0.09 (7.1)	0.69 ± 0.13 (5.4)	AGN	34,29	WKK 6471; Sy1 z=0.035;
146	IGR J16195-4945	244.881	-49.741	2.10 ± 0.09	1.44 ± 0.07	0.85 ± 0.09 (9.2)	HMXB	60,61	AX J161929-4945;
147	IGR J16195-2807	244.882	-28.132	2.72 ± 0.23	1.88 ± 0.17	1.36 ± 0.22 (6.1)	LMXB	26,62	SyXB; IRXS J161933.6-280736; ↴
148	IGR J16207-5129	245.194	-51.503	3.78 ± 0.10	2.27 ± 0.07	1.84 ± 0.09	HMXB	60,61	
149	4U 1624-49	247.006	-49.203	4.44 ± 0.09	4.02 ± 0.07	0.23 ± 0.09 (2.5)	LMXB	60,61	
150	IGR J16283-4838	247.068	-48.659	0.84 ± 0.09 (8.9)	0.53 ± 0.07 (8.1)	0.36 ± 0.09 (3.9)	HMXB	63,64	

Table 2. Continued.

Id	Name	RA [†] deg	Dec [‡] deg	F _{17–60 keV} [*] erg cm ⁻² s ⁻¹	F _{7–35 keV} [*] erg cm ⁻² s ⁻¹	F _{35–80 keV} [*] erg cm ⁻² s ⁻¹	Type	Ref. ^{**}	Notes ^{***}
151	IGR J16287-5021	247.125	-50.368	0.55 ± 0.09 (5.8)	0.52 ± 0.07 (7.9)	< 0.19	LMXB	12	
152	IGR J16293-4603	247.369	-46.081	0.56 ± 0.10 (5.8)	0.33 ± 0.07 (4.9)	0.19 ± 0.09 (2.0)	LMXB	65,66	SyXB?
153	IGR J16318-4848	247.952	-48.816	29.84 ± 0.09	18.59 ± 0.07	13.12 ± 0.09	HMXB	67,68	AX J1631.9-4752
154	IGR J16320-4751	248.008	-47.877	20.98 ± 0.09	14.60 ± 0.07	6.54 ± 0.09	HMXB	69,70	
155	4U 1626-67	248.075	-67.465	21.36 ± 0.21	17.50 ± 0.14	2.82 ± 0.22	LMXB		C157; C156,159;
156	IGR J16336-4733	248.396	-47.559	4.80 ± 0.09	2.80 ± 0.07	2.69 ± 0.09	LMXB		Sy2 z=0.009113; C157; symbiotic X-ray binary z=0.051; IRXSI16330.9-205520; ↴ ↳ Sy1 z=0.0269;
157	4U 1630-47	248.524	-47.390	24.29 ± 0.09	14.52 ± 0.07	13.71 ± 0.09	LMXB	71,72	
158	ESO 137-G34	248.829	-58.085	1.19 ± 0.12 (9.6)	0.65 ± 0.09 (7.5)	0.95 ± 0.12 (7.6)	AGN		
159	IGR J16558-4726	248.992	-47.407	0.89 ± 0.09 (9.4)	0.49 ± 0.07 (7.4)	0.49 ± 0.09 (5.3)	LMXB		
160	Triangulum A	249.546	-64.377	1.45 ± 0.19 (7.6)	1.05 ± 0.13 (8.1)	0.41 ± 0.19 (2.1)	Cluster		
161	IGR J16385-2057	249.643	-20.914	0.93 ± 0.17 (5.5)	0.65 ± 0.13 (5.0)	0.61 ± 0.15 (4.0)	AGN		
162	AX J163904-4642	249.774	-46.705	6.08 ± 0.10	4.95 ± 0.07	0.98 ± 0.09	HMXB	73	
163	4U 1636-536	250.229	-53.754	30.36 ± 0.10	20.66 ± 0.07	12.02 ± 0.10	LMXB		
164	IGR J16418-4532	250.463	-45.536	4.91 ± 0.10	3.42 ± 0.07	1.63 ± 0.09	HMXB	74,75	
165	GX 340+0	251.448	-45.613	37.46 ± 0.10	34.17 ± 0.07	1.66 ± 0.09	LMXB		
166	IGR J16465-4507	251.648	-45.118	1.66 ± 0.10	1.21 ± 0.07	0.61 ± 0.09 (6.4)	HMXB	76,77	C167;
167	IGR J16479-4514	252.023	-45.210	4.87 ± 0.10	3.11 ± 0.07	2.15 ± 0.09	HMXB	78,79	2MASS J16480656-4512068; Sy1 z=0.031; ↴
168	IGR J16482-3036	252.053	-30.575	2.32 ± 0.11	1.27 ± 0.08	1.79 ± 0.12	AGN	26,37	2MASS J16492695-3035037; IP, 1RXS J164955.1-330713; Sy2 z=0.004750; ↴
169	IGR J16493-4348	252.369	-43.822	2.60 ± 0.10	1.59 ± 0.07	1.38 ± 0.10	HMXB	80,81	↳ May contain flux from ESO 138-G1; Black hole candidate;
170	IGR J16500-3307	252.488	-33.113	1.75 ± 0.11	1.27 ± 0.07	0.62 ± 0.11 (5.7)	HMXB	26,1	
171	NGC 6221	253.048	-59.219	1.69 ± 0.14	1.02 ± 0.10	0.92 ± 0.14 (6.4)	AGN		
172	XTE J1652-453	253.075	-45.345	1.73 ± 0.10	1.04 ± 0.07	1.01 ± 0.09	LMXB?	82	
173	GRO J1655-40	253.499	-39.845	10.41 ± 0.10	5.69 ± 0.07	7.14 ± 0.10	LMXB		
174	IGR J16547-1916	253.706	-19.269	1.33 ± 0.14 (9.3)	1.02 ± 0.11 (9.6)	0.61 ± 0.14 (4.3)	CV	12,83	IP; RXS J165443.5-191620;
175	IGR J16560-4958	253.963	-49.987	0.54 ± 0.10 (5.4)	0.25 ± 0.07 (3.6)	0.44 ± 0.10 (4.5)	AGN	60,29	Sy1,2 z=0.054;
176	IGR J16558-5203	254.034	-52.081	2.13 ± 0.11	1.16 ± 0.07	1.50 ± 0.10	AGN	84	BL Lac; SWIFT J1656.3-3302;
177	IGR J16562-3301	254.089	-33.038	2.23 ± 0.09	1.13 ± 0.07	1.83 ± 0.10	AGN	85	Black hole candidate;
178	MAXI J1659-152	254.761	-15.256	14.61 ± 0.17	9.59 ± 0.13	6.67 ± 0.16	HMXB	46	
179	AX J1700.2-4220	255.077	-42.338	1.61 ± 0.10	0.93 ± 0.07	0.76 ± 0.10 (8.0)	HMXB		
180	OAO 1657-415	255.203	-41.655	82.92 ± 0.10	53.23 ± 0.07	35.96 ± 0.09	HMXB		
181	XTE J1701-462	255.243	-46.195	3.22 ± 0.10	2.98 ± 0.07	< 0.19	HMXB		
182	IGR J17014-4306	255.337	-43.092	0.72 ± 0.10 (7.2)	0.46 ± 0.07 (6.6)	0.34 ± 0.10 (3.6)	Star		SWIFT J1701.3-4304; ↴ ↳ 2MASS J17012815-4306123;
183	XTE J1701-407	255.415	-40.868	3.19 ± 0.10	1.83 ± 0.07	2.01 ± 0.10	LMXB	86	
184	GX 339-4	255.707	-48.790	102.50 ± 0.10	55.41 ± 0.07	70.55 ± 0.10	LMXB		
185	4U 1700-377	255.985	-37.845	247.76 ± 0.09	158.55 ± 0.06	111.86 ± 0.09	HMXB		
186	GX 349+2	256.434	-36.420	52.33 ± 0.09	48.61 ± 0.06	0.91 ± 0.09	LMXB	87,88	=SWIFT J1706.6-6146
187	IGR J17062-6143	256.562	-61.703	2.00 ± 0.19	1.17 ± 0.13 (9.2)	1.21 ± 0.19 (6.4)	LMXB		
188	4U 1702-429	256.565	-43.036	16.36 ± 0.10	10.96 ± 0.07	6.84 ± 0.10	AXP		
189	IRXS J170849.0-400910	257.204	-40.149	1.45 ± 0.09	0.75 ± 0.06	1.18 ± 0.09	LMXB		
190	4U 1705-440	257.228	-44.104	23.03 ± 0.10	17.22 ± 0.07	6.86 ± 0.10	LMXB		
191	4U 1705-32	257.229	-32.320	1.93 ± 0.08	1.17 ± 0.05	1.10 ± 0.08	LMXB		
192	IGR J17091-3624	257.289	-36.405	8.96 ± 0.08	4.70 ± 0.06	6.27 ± 0.09	LMXB	89,90	C194;
193	XTE J1709-267	257.399	-26.654	0.99 ± 0.08	0.61 ± 0.06	0.58 ± 0.08 (7.0)	LMXB	91,92	C192;
194	IGR J17098-3628	257.485	-36.448	5.57 ± 0.08	2.99 ± 0.06	3.70 ± 0.09	LMXB?		

Table 2. Continued.

Id	Name	RA [†] deg	Dec [‡] deg	F _{17–60 keV} [*] erg cm ⁻² s ⁻¹	F _{17–35 keV} [*] erg cm ⁻² s ⁻¹	F _{35–80 keV} [*] erg cm ⁻² s ⁻¹	Type	Ref. ^{**}	Notes ^{***}
195	XTE J1710-281	257.552	-28.132	3.13 ± 0.08	1.77 ± 0.05	1.97 ± 0.08	LMXB		
196	RX J1713.7-3946	258.042	-39.921	0.48 ± 0.09 (5.3)	0.34 ± 0.06 (5.4)	0.21 ± 0.09 (2.3)	SNR		G347.3-0.5; extended source;
197	4U1708-40	258.115	-40.841	0.80 ± 0.09 (8.6)	0.90 ± 0.06	< 0.19	LMXB		
198	Oph cluster	258.116	-23.348	4.83 ± 0.09	3.94 ± 0.06	0.81 ± 0.09 (8.9)	Cluster		
199	V2400 Oph	258.153	-24.247	3.24 ± 0.08	2.30 ± 0.06	1.04 ± 0.09	CV		
200	SAXJ1712.6-3739	258.156	-37.643	5.55 ± 0.08	3.34 ± 0.06	3.03 ± 0.09	LMXB		
201	IGR J17157-5449	258.924	-54.805	0.72 ± 0.13 (5.5)	0.34 ± 0.09 (3.8)	0.54 ± 0.13 (4.2)			IRXS J171535 6-545015; ↴ ↳ HD 155573 (Landi et al., 2012);
202	IGR J17164-3803	259.123	-38.040	0.87 ± 0.08	0.66 ± 0.06	0.31 ± 0.09 (3.6)	AGN		Sy2 z=0.003706;
203	NGC 6300	259.254	-62.819	5.38 ± 0.21	2.95 ± 0.14	3.44 ± 0.22			
204	IGR J17174-2436	259.335	-24.606	0.64 ± 0.08 (8.2)	0.43 ± 0.05 (8.0)	0.24 ± 0.08 (3.0)	LMXB	93	Symbiotic binary IRXS J171935.6-410054;
205	IGR J17197-3010	259.889	-30.172	0.40 ± 0.07 (5.8)	0.24 ± 0.05 (5.0)	0.21 ± 0.07 (3.0)	CV	60,46	
206	IGR J17195-4100	259.906	-41.015	2.57 ± 0.09	1.79 ± 0.06	1.02 ± 0.10	LMXB		
207	XTE J1720-318	259.998	-31.759	0.91 ± 0.07	0.45 ± 0.05 (9.5)	0.63 ± 0.07 (8.9)	HMXB		IRXS J172006.1-311702;
208	IGR J17200-3116	260.021	-31.285	2.15 ± 0.07	1.55 ± 0.05	0.58 ± 0.07 (8.2)	HMXB	60,29	
209	IGR J17204-3554	260.094	-35.912	0.69 ± 0.08 (9.2)	0.37 ± 0.05 (7.0)	0.51 ± 0.08 (6.6)	AGN	26,94	
210	IGR J17233-2837	260.850	-28.622	0.64 ± 0.07 (9.7)	0.35 ± 0.05 (7.6)	0.44 ± 0.07 (6.4)			IRXS J172323.7-283805
211	EXO 1722-363	261.297	-36.284	9.21 ± 0.07	6.66 ± 0.05	2.52 ± 0.08	HMXB		
212	IGR J17254-3257	261.353	-32.964	1.98 ± 0.07	1.16 ± 0.05	1.10 ± 0.07	LMXB	60,95	IRXS J172525.5-325717;
213	4U 1724-30	261.887	-30.800	22.45 ± 0.06	13.39 ± 0.04	11.98 ± 0.07	LMXB		Terzan 2; IRXS J173021.5-055933;
214	IGR J17303-0601	262.588	-5.984	4.24 ± 0.17	2.56 ± 0.11	2.18 ± 0.19	CV	60,96	
215	IGR J17306-2015	262.601	-20.272	1.60 ± 0.09	1.02 ± 0.06	0.71 ± 0.09 (7.9)			
216	IGR J17315-3221	262.818	-32.306	0.43 ± 0.06 (6.6)	0.34 ± 0.04 (7.6)	< 0.13	HMXB		
217	GX 9+9	262.936	-16.957	13.11 ± 0.11	12.21 ± 0.08	0.41 ± 0.11 (3.6)	LMXB		
218	GX 354+0	262.991	-33.833	56.28 ± 0.07	40.00 ± 0.05	19.36 ± 0.07	LMXB		
219	GX 1+4	263.011	-24.743	71.47 ± 0.07	40.77 ± 0.05	40.93 ± 0.07	LMXB		
220	IGR J17320-1914	263.013	-19.209	0.94 ± 0.09	0.59 ± 0.06 (9.3)	0.45 ± 0.10 (4.7)	CV	4	V2487 Oph;
221	IGR J17331-2406	263.250	-24.147	0.48 ± 0.07 (7.0)	0.25 ± 0.05 (5.2)	0.31 ± 0.07 (4.4)	LMXB	97	
222	RapidBurster	263.351	-33.391	4.18 ± 0.07	3.21 ± 0.05	1.05 ± 0.07	AGN?	45	2MASS J17345863-2045292; ↴ ↳ Radio source;
223	IGR J17350-2045	263.746	-20.745	0.91 ± 0.08	0.49 ± 0.06 (8.7)	0.73 ± 0.08 (8.7)			
224	IGR J17353-3539	263.848	-35.670	0.91 ± 0.07	0.60 ± 0.05	0.34 ± 0.07 (4.6)	LMXB	98	
225	IGR J17353-3257	263.856	-32.921	1.37 ± 0.06	0.78 ± 0.04	0.68 ± 0.07	HMXB	99,51	intermediate SFXT; ↴ ↳ =IGR J17354-3255;
226	IGR J17361-4444	264.076	-44.738	0.58 ± 0.11 (5.1)	0.26 ± 0.08 (3.3)	0.39 ± 0.12 (3.2)	LMXB?	100,101	=IGR J17361-4444;
227	GRS 1734-292	264.370	-29.134	6.36 ± 0.06	3.71 ± 0.04	3.70 ± 0.06	HMXB		Sy1 z=0.021400;
228	IGR J17379-5957	264.397	-59.956	1.04 ± 0.20 (5.2)	0.64 ± 0.14 (4.7)	0.59 ± 0.20 (3.0)	AGN		Sy2 z=0.0174; ESO 139-12;
229	SLX 1735-269	264.572	-26.992	13.64 ± 0.06	7.99 ± 0.04	7.73 ± 0.06	LMXB		
230	4U 1735-444	264.744	-44.452	26.78 ± 0.12	24.63 ± 0.08	1.13 ± 0.12 (9.3)	LMXB		
231	IGR J17391-3021	264.802	-30.347	1.07 ± 0.06	0.69 ± 0.04	0.35 ± 0.06 (5.5)	HMXB	102,103	=XTE J1739-302;
232	GRS 1736-297	264.880	-29.707	0.31 ± 0.06 (5.1)	0.17 ± 0.04 (4.1)	0.18 ± 0.06 (2.9)	LMXB		C235;
233	XTE J1739-285	264.975	-28.496	1.60 ± 0.06	1.02 ± 0.04	0.85 ± 0.06	LMXB	51	=IGR J17404-3655;
234	IGR J17402-3656	265.104	-36.925	0.85 ± 0.08	0.46 ± 0.05 (8.9)	0.41 ± 0.08 (5.3)	HMXB?		C233,C236;
235	SLX 1737-282	265.168	-28.313	4.53 ± 0.06	2.62 ± 0.04	2.70 ± 0.06	LMXB		CXOU J174042.0-280724
236	IGR J17407-2808	265.175	-28.133	1.45 ± 0.06	0.80 ± 0.04	0.99 ± 0.06	LMXB?	104,105	2E 1739.1-1210; Sy1 z=0.037;
237	IGR J17418-1212	265.487	-12.201	2.04 ± 0.13	1.11 ± 0.09	1.43 ± 0.14	AGN	106,107	SFXT? Quasar z=1.054; ↴
238	XTE J1743-363	265.744	-36.380	2.43 ± 0.07	1.59 ± 0.05	0.98 ± 0.08	HMXB		
239	IGR J17438-0347	265.952	-3.787	0.79 ± 0.14 (5.5)	0.27 ± 0.10 (2.8)	0.42 ± 0.16 (2.6)	AGN		

Table 2. Continued.

Id	Name	RA [†] deg	Dec [‡] deg	F _{17–60 keV} [*] erg cm ⁻² s ⁻¹	F _{17–35 keV} [*] erg cm ⁻² s ⁻¹	F _{35–80 keV} [*] erg cm ⁻² s ⁻¹	Type	Ref. ^{**}	Notes ^{***}
240	IE 1740.7-294	265.984	-29.735	46.31 ± 0.06	24.52 ± 0.04	33.19 ± 0.06	LMXB	108	L _↑ QSO B1741-038; C242,246;
241	IGR J17448-3231	266.190	-32.528	0.53 ± 0.06 (8.5)	0.43 ± 0.04 (9.9)	0.13 ± 0.07 (2.1)	AGN?		C247; CXOU J174437.3-323222; ↓
242	KS1741-293	266.242	-29.337	4.73 ± 0.06	2.98 ± 0.04	2.32 ± 0.06	LMXB		↑ Blazar (?); C240;
243	GRS 1741.9-2853	266.250	-28.917	4.10 ± 0.06	2.78 ± 0.04	1.70 ± 0.06	LMXB		C244,245,248,249;
244	AX J1745.6-2901	266.401	-29.026	7.18 ± 0.06	4.82 ± 0.04	3.11 ± 0.06	NucStrCl	109,110	C242,243,245,248,249; ↓ ↑ =IGR J17456-2901; ↓ Nuclear stellar cluster; C243,244,248,249;
245	IE 1742.8-2853	266.500	-28.914	7.46 ± 0.06	5.05 ± 0.04	3.16 ± 0.06	LMXB		C240;
246	A 1742-294	266.525	-29.518	15.51 ± 0.06	10.72 ± 0.04	5.87 ± 0.06	LMXB		H1743-322/XTE J1746-322;
247	IGR J17464-3213	266.566	-32.233	21.03 ± 0.06	12.63 ± 0.04	11.83 ± 0.06	LMXB	111	C249,245;
248	IE 1743.1-2843	266.580	-28.735	5.94 ± 0.06	4.41 ± 0.04	1.80 ± 0.06	LMXB		C243,244,245,248;
249	SAX J1747.0-2853	266.761	-28.883	3.51 ± 0.06	2.40 ± 0.04	1.35 ± 0.06	LMXB		C233; Neutron star LMXB
250	IGR J17464-2811	266.817	-28.180	1.98 ± 0.06	1.22 ± 0.04	0.99 ± 0.06	LMXB	112,113	
251	IGR J17473-2721	266.826	-27.349	2.90 ± 0.06	1.62 ± 0.04	1.78 ± 0.06	LMXB	114,115	C246;
252	SLX1744-299/300	266.834	-30.010	9.92 ± 0.06	6.62 ± 0.04	4.31 ± 0.06	LMXB		C250; SgrB2;
253	IGR J17475-2822	266.868	-28.370	2.60 ± 0.06	1.57 ± 0.04	1.31 ± 0.06	MolCld	116	Sy _v z=0.0463; ↓ ↑ IGR J17476-2253;
254	IGR J17475-2253	266.896	-22.872	1.02 ± 0.07	0.56 ± 0.05	0.58 ± 0.07 (8.2)	AGN	117	C259;
255	GX 3+1	266.984	-26.556	14.56 ± 0.06	13.38 ± 0.04	0.49 ± 0.06 (7.7)	LMXB		Sy _v z=0.020;
256	IGR J17488-3253	267.223	-32.918	1.64 ± 0.06	0.87 ± 0.04	1.25 ± 0.07	AGN	60,29	C258;
257	AX J1749.1-2733	267.275	-27.550	1.55 ± 0.06	0.97 ± 0.04	0.71 ± 0.06	HMXB	118,119	C257;
258	AX J1749.2-2725	267.292	-27.421	1.21 ± 0.06	0.72 ± 0.04	0.62 ± 0.06 (9.8)	HMXB	120	C255;
259	GRO J1750.27	267.300	-26.647	5.57 ± 0.06	4.78 ± 0.04	0.56 ± 0.06 (8.8)	HMXB		
260	IGR J17497-2821	267.399	-28.352	2.91 ± 0.06	1.60 ± 0.04	2.02 ± 0.06	LMXB	121,122	Black hole X-ray transient; IGR J17507-2647
261	SLX 1746-331	267.475	-33.215	0.60 ± 0.06 (9.3)	0.32 ± 0.04 (7.2)	0.36 ± 0.07 (5.3)	LMXB		
262	4U 1746-37	267.552	-37.054	2.94 ± 0.08	2.54 ± 0.05	0.26 ± 0.08 (3.2)	LMXB		
263	SAX J1750.8-2900	267.600	-29.038	1.51 ± 0.06	1.01 ± 0.04	0.75 ± 0.06	LMXB		
264	IGR J17505-2644	267.658	-26.734	0.72 ± 0.06	0.50 ± 0.04	0.28 ± 0.06 (4.4)	LMXB?	123	
265	IGR J17507-2856	267.683	-28.922	0.71 ± 0.06	0.52 ± 0.04	0.39 ± 0.06 (6.3)	LMXB		
266	GRS 1747-313	267.695	-31.284	1.39 ± 0.06	0.99 ± 0.04	0.50 ± 0.06 (7.9)	LMXB		
267	XTE J1751-305	267.815	-30.639	0.31 ± 0.06 (5.0)	0.11 ± 0.04 (2.5)	0.25 ± 0.06 (4.0)	LMXB		
268	IGR J17513-2011	267.825	-20.211	1.23 ± 0.08	0.67 ± 0.05	0.95 ± 0.08	AGN	26,29	Sy _v z=0.047;
269	XTE J1752-223	268.064	-22.349	1.48 ± 0.07	0.75 ± 0.05	1.14 ± 0.07	LMXB		Black hole candidate;
270	SWIFT J1753.5-0127	268.367	-1.451	85.67 ± 0.14	44.64 ± 0.09	64.18 ± 0.16	LMXB		
271	AX J1753.5-2745	268.375	-27.750	0.29 ± 0.06 (4.8)	0.19 ± 0.04 (4.6)	0.27 ± 0.06 (4.2)	LMXB	125	
272	AX J1754.2-2754	268.566	-27.887	0.49 ± 0.06 (8.1)	0.31 ± 0.04 (7.3)	0.23 ± 0.06 (3.6)	HMXB	126,127	
273	IGR J17544-2619	268.601	-26.322	0.86 ± 0.06	0.67 ± 0.04	0.44 ± 0.07 (6.7)	LMXB?	128	
274	IGR J17585-3057	269.599	-30.961	0.65 ± 0.06	0.36 ± 0.04 (8.4)	0.79 ± 0.08	LMXB?	51	
275	IGR J17586-2129	269.654	-21.382	2.15 ± 0.07	1.38 ± 0.05	2.04 ± 0.08	LMXB	129,130	XTE J1759-220; AM Herculis
276	IGR J17597-2201	269.936	-22.018	3.95 ± 0.07	2.40 ± 0.05				
277	V2301 OPH	270.149	8.185	1.30 ± 0.23 (5.8)	0.87 ± 0.15 (5.8)	< 0.51	CV		
278	GX 5-1	270.285	-25.078	61.84 ± 0.07	55.79 ± 0.05	2.83 ± 0.07	LMXB		
279	GRS 1758-258	270.303	-25.744	65.69 ± 0.06	33.74 ± 0.04	49.71 ± 0.07	LMXB		
280	GX 9+1	270.387	-20.517	21.49 ± 0.08	19.98 ± 0.05	0.26 ± 0.08 (3.2)	LMXB		
281	IGR J18027-2016	270.677	-20.278	5.71 ± 0.08	4.11 ± 0.05	1.51 ± 0.08	HMXB	131,132	C281;
282	IGR J18027-1455	270.696	-14.911	2.17 ± 0.10	1.18 ± 0.07	1.51 ± 0.11	AGN	60,133	C280; IGR/SAX J18027-2017; Sy _v z=0.0350; ↓

Table 2. Continued.

Id	Name	RA [†] deg	Dec [‡] deg	F _{17-60 keV} [*] erg cm ⁻² s ⁻¹	F _{17-35 keV} [*] erg cm ⁻² s ⁻¹	F _{35-80 keV} [*] erg cm ⁻² s ⁻¹	Type	Ref. ^{**}	Notes ^{***}
283	IGR J18044-2739	271.115	-27.671	0.67 ± 0.06	0.40 ± 0.04 (9.0)	0.32 ± 0.07 (4.8)	LMXB	134	↪ RXS J180245.2-14542;
284	IGR J18048-1455	271.179	-14.958	0.86 ± 0.10 (8.6)	0.60 ± 0.07 (8.7)	0.28 ± 0.11 (2.6)	LMXB	26,45	↪ RXP J180431.1-273932
285	XTE J1807-294	271.755	-29.436	0.54 ± 0.06 (8.4)	0.32 ± 0.04 (7.0)	0.35 ± 0.07 (5.1)	LMXB	12	Sy1.2 z=0.078 ms pulsar
286	IGR J18078+1123	271.939	11.369	1.20 ± 0.24 (5.0)	0.80 ± 0.16 (4.9)	0.64 ± 0.27 (2.4)	AGN		
287	SAX J1808-3658	272.106	-36.982	0.71 ± 0.09 (8.3)	0.47 ± 0.06 (8.0)	0.56 ± 0.09 (6.3)	LMXB		
288	SGR 1806-20	272.169	-20.413	2.97 ± 0.08	1.54 ± 0.06	2.18 ± 0.08	SGR		
289	IGR J18088-2741	272.254	-27.704	0.59 ± 0.07 (9.0)	0.42 ± 0.05 (9.2)	0.20 ± 0.07 (2.9)	Burster;		
290	XTE J1810-189	272.586	-19.069	2.12 ± 0.09	1.23 ± 0.06	1.22 ± 0.09	LMXB		
291	V4722 Sgr	272.693	-26.148	2.73 ± 0.07	1.57 ± 0.05	1.60 ± 0.07	LMXB		
292	PSR J1811-1925	272.872	-19.423	0.96 ± 0.08	0.46 ± 0.06 (7.8)	0.75 ± 0.09 (8.4)	PSR/PWN		SNR G11.2-0.3;
293	IGR J18134-1636	273.373	-16.620	0.82 ± 0.10 (8.6)	0.44 ± 0.07 (6.7)	0.59 ± 0.10 (5.8)			
294	IGR J18135-1751	273.398	-17.839	1.57 ± 0.09	0.85 ± 0.06	1.06 ± 0.10	SNR/PWN	135,136	HESS J1813-178;
295	GX 13+1	273.631	-17.158	13.71 ± 0.09	11.92 ± 0.06	1.53 ± 0.10	LMXB		
296	M 1812-12	273.776	-12.096	34.25 ± 0.10	19.07 ± 0.07	21.63 ± 0.11	LMXB		
297	GX 17+2	274.006	-14.035	69.43 ± 0.10	62.21 ± 0.07	3.75 ± 0.11	LMXB		
298	IGR J18170-2511	274.303	-25.152	1.08 ± 0.07	0.79 ± 0.05	0.31 ± 0.08 (4.0)	CV	8	IP; =IGR J18173-2509;
299	IGR J18175-1530	274.392	-15.468	0.47 ± 0.10 (4.8)	0.27 ± 0.07 (3.9)	0.25 ± 0.11 (2.3)	LMXB	137	
300	XTE J1817-330	274.427	-33.021	5.13 ± 0.08	3.21 ± 0.05	2.58 ± 0.08	LMXB?		
301	XTE J1818-245	274.618	-24.523	3.29 ± 0.08	2.05 ± 0.05	1.89 ± 0.08	LMXB?		
302	SAX J1818.6-1703	274.687	-17.046	1.56 ± 0.10	1.04 ± 0.07	0.69 ± 0.10 (6.7)	HMXB	1	
303	AX J1820.5-1434	275.136	-14.571	1.79 ± 0.10	1.18 ± 0.07	0.70 ± 0.11 (6.3)	HMXB		
304	IGR J18214-1318	275.328	-13.315	1.85 ± 0.10	1.14 ± 0.07	1.09 ± 0.11 (9.7)	HMXB?	26,138	
305	IGR J18219-1347	275.504	-13.803	0.71 ± 0.10 (6.9)	0.50 ± 0.06 (7.2)	< 0.22	HMXB?	45	
306	4U 1820-303	275.917	-30.364	40.48 ± 0.08	36.14 ± 0.05	2.28 ± 0.08	LMXB		
307	XTE J1824-141	276.116	-14.429	0.93 ± 0.10 (9.0)	0.55 ± 0.07 (7.9)	0.30 ± 0.11 (2.7)	HMXB?	139	X-Ray Pulsar; ↪
308	IGR J18249-3243	276.214	-32.726	0.82 ± 0.08 (9.8)	0.50 ± 0.06 (8.6)	0.57 ± 0.09 (6.5)	AGN	140,8	↪ =IGR J18246-1425;
309	4U 1822-000	276.333	-0.007	1.87 ± 0.11	1.67 ± 0.07	< 0.24	LMXB		Sy1 z=0.355; PKS 1821-327?;
310	IGR J18256-1035	276.428	-10.594	0.73 ± 0.10 (7.2)	0.52 ± 0.07 (7.6)	< 0.23			Sy1 z=0.358; PKS 1821-327?;
311	4U 1822-371	276.446	-37.108	32.87 ± 0.10	27.07 ± 0.07	4.45 ± 0.11	LMXB		
312	IGR J18257-0707	276.478	-7.161	1.00 ± 0.10	0.60 ± 0.07 (8.9)	0.63 ± 0.11 (5.7)	AGN	26,42	Sy1 z=0.037; ↪
313	LS 5039	276.551	-14.847	1.03 ± 0.10	0.57 ± 0.07 (8.1)	0.88 ± 0.11 (7.8)	HMXB		
314	IGR J18293-1213	277.318	-12.214	0.76 ± 0.10 (7.3)	0.50 ± 0.07 (7.1)	0.45 ± 0.11 (3.9)			
315	GS 1826-24	277.370	-23.798	106.43 ± 0.09	62.40 ± 0.06	60.26 ± 0.09	LMXB		
316	AX J183039-1002	277.648	-10.032	0.97 ± 0.10 (9.6)	0.58 ± 0.07 (8.5)	0.43 ± 0.11 (3.8)	AGN?	141	
317	IGR J18308-1232	277.700	-12.538	0.97 ± 0.10 (9.4)	0.58 ± 0.07 (8.3)	0.47 ± 0.11 (4.1)	CV	51	IGR J18307-1232
318	AX J1832.3-0840	278.082	-8.640	0.62 ± 0.10 (6.2)	0.48 ± 0.07 (7.1)	< 0.22	HMXB?	142,42	
319	IGR J18293-1213	278.110	-7.951	1.45 ± 0.10	0.78 ± 0.07	0.80 ± 0.11 (7.2)			
320	SNR 021.5-00.9	278.386	-10.569	3.73 ± 0.10	2.11 ± 0.07	2.31 ± 0.11	SNR		
321	PKS 1830-211	278.420	-21.058	2.83 ± 0.10	1.37 ± 0.07	2.19 ± 0.11	AGN		
322	3C382	278.783	32.698	3.92 ± 0.53 (7.4)	2.13 ± 0.36 (5.9)	3.12 ± 0.58 (5.4)	LMXB		
323	RX J1832-33	278.933	-32.993	12.15 ± 0.10	6.72 ± 0.07	7.83 ± 0.11	SNR/PWN		Quasar z=2.507; Sy1 z=0.058137;
324	AX J1838.0-0655	279.507	-6.920	2.55 ± 0.10	1.36 ± 0.07	2.12 ± 0.11			
325	IGR J18381-0924	279.538	-9.415	0.60 ± 0.10 (5.9)	0.30 ± 0.07 (4.3)	0.40 ± 0.11 (3.5)	HESS	143	HESS J1837-069;
326	Ser X-1	279.988	5.039	12.42 ± 0.10	11.29 ± 0.07	0.37 ± 0.11 (3.3)	LMXB		
327	IGR J18400-2439	280.055	-24.634	0.66 ± 0.11 (6.2)	0.46 ± 0.07 (6.2)	< 0.22			

Table 2. Continued.

Id	Name	RA [†] deg	Dec [‡] deg	F _{17–60 keV} [*] erg cm ⁻² s ⁻¹	F _{7–35 keV} [*] erg cm ⁻² s ⁻¹	F _{35–80 keV} [*] erg cm ⁻² s ⁻¹	Type	Ref. ^{**}	Notes ^{***}
328	IGR J18410-0535	280.259	-5.593	0.95 ± 0.10 (9.5)	0.54 ± 0.07 (8.0)	0.62 ± 0.11 (5.6)	HMXB	144,145	AX J1841.0-0536;
329	IE1841-045	280.333	-4.939	3.24 ± 0.10	1.42 ± 0.07	2.95 ± 0.11	PSR/PWN		
330	AX J1845.0-0433	281.263	-4.567	1.69 ± 0.10	1.04 ± 0.07	0.76 ± 0.11 (6.8)	HMXB		
331	GS 1843+00	281.404	0.865	5.26 ± 0.10	3.16 ± 0.06	2.63 ± 0.10	PSR/PWN		
332	PSR J1846-0258	281.602	-2.973	2.14 ± 0.10	1.15 ± 0.07	1.58 ± 0.11	HMXB		AXP?
333	A 1845-024	282.044	-2.427	0.69 ± 0.10 (7.1)	0.33 ± 0.07 (5.0)	0.53 ± 0.11 (4.9)	PSR/PWN		
334	IGR J18483-0311	282.071	-3.172	5.56 ± 0.10	3.61 ± 0.07	2.43 ± 0.11	HMXB	146,79	SFXT
335	IGR J18486-0047	282.102	-0.776	1.10 ± 0.10	0.69 ± 0.06	0.51 ± 0.10 (5.0)	AGN?	51	strong radio source; ↳ high X-ray abs.; =IGR J18485-0047;
336	IGR J18490-0000	282.257	-0.026	1.45 ± 0.09	0.82 ± 0.06	0.94 ± 0.10 (9.0)	PWN	147,148	NVSS J184946.9-024819; ↳
337	IGR J18497-0248	282.436	-2.863	0.52 ± 0.10 (5.3)	0.20 ± 0.07 (3.0)	0.55 ± 0.11 (5.0)	PWN	149	Radio source; ↳ SWIFT J184946.9-024813;
338	4U 1850-087	283.271	-8.706	6.36 ± 0.11	3.80 ± 0.07	3.67 ± 0.12	LMXB		
339	IGR J18538-0102	283.452	-1.047	0.52 ± 0.10 (5.5)	0.26 ± 0.06 (4.0)	0.28 ± 0.11 (2.7)	AGN	18	Sy1 z=0.145; V1223 Sgr;
340	4U 1849-31	283.761	-31.160	7.88 ± 0.14	5.38 ± 0.10	3.08 ± 0.15	CV		
341	XTE J1855-026	283.876	-2.602	12.39 ± 0.10	7.75 ± 0.07	5.79 ± 0.11	HMXB		
342	IGR J18559+1535	283.986	15.641	1.72 ± 0.11	1.01 ± 0.08	0.96 ± 0.12 (7.8)	AGN	150	Sy1 z=0.084; 2E 1853.7+1534;
343	XTE J1858+034	284.680	3.438	6.73 ± 0.09	5.55 ± 0.06	0.98 ± 0.10	HMXB		
344	HETE J19001-2455	285.039	-24.921	23.59 ± 0.16	13.43 ± 0.11	14.27 ± 0.18	LMXB		
345	XTE J1901+014	285.416	1.442	3.31 ± 0.09	2.04 ± 0.06	1.83 ± 0.10	LMXB	151	
346	4U 1901+03	285.914	3.206	16.89 ± 0.09	14.12 ± 0.06	2.05 ± 0.10	HMXB		
347	IGR J19072-2046	286.807	-20.765	1.13 ± 0.17 (6.8)	0.87 ± 0.11 (7.8)	< 0.37	CV		
348	SGR 1900+14	286.837	9.328	1.13 ± 0.08	0.60 ± 0.06	0.69 ± 0.09 (7.5)	SGR		
349	XTE J1908+094	287.217	9.378	0.77 ± 0.08 (9.1)	0.36 ± 0.06 (6.3)	0.63 ± 0.09 (6.8)	LMXB		
350	4U 1907+097	287.411	9.832	15.07 ± 0.08	12.61 ± 0.06	1.81 ± 0.09	HMXB		
351	X1908+075	287.702	7.600	16.91 ± 0.08	11.11 ± 0.06	7.48 ± 0.09	LMXB		
352	Aql X-1	287.816	0.583	13.62 ± 0.09	8.05 ± 0.06	7.64 ± 0.10	LMXB		
353	IGR J19113+1413	287.835	14.225	0.87 ± 0.10 (9.1)	0.55 ± 0.07 (8.4)	0.28 ± 0.11 (2.6)	LMXB		
354	SS 433	287.957	4.985	10.74 ± 0.08	7.11 ± 0.06	4.41 ± 0.09	HMXB		
355	IGR J19140+0951	288.517	9.884	11.17 ± 0.09	7.13 ± 0.06	5.13 ± 0.09	HMXB	152,132	=IGR J19140+098;
356	GRS 1915+105	288.799	10.945	337.72 ± 0.09	236.40 ± 0.06	122.31 ± 0.10	LMXB		
357	4U 1916-053	289.692	-5.240	10.56 ± 0.12	6.93 ± 0.08	4.94 ± 0.14	LMXB		
358	IGR J19267+1325	291.645	13.405	0.53 ± 0.10 (5.5)	0.38 ± 0.07 (5.8)	4.41 ± 0.09	HMXB		
359	IGR J19302+3411	292.535	34.164	1.25 ± 0.17 (7.5)	0.71 ± 0.11 (6.2)	0.65 ± 0.18 (3.7)	AGN	20	Sy1 z=0.06326; ↳
360	SWIFT J1933.9+3258	293.460	32.905	1.47 ± 0.16 (9.4)	0.98 ± 0.11 (9.2)	0.76 ± 0.17 (4.6)	AGN	154	IRXS J19266.8+132153 Sy1 z=0.005214; =SWIFT J1930.5+3414; ↳ =RXS J193347.6+325422;
361	IH 1934-063	294.377	-6.227	1.40 ± 0.16 (8.7)	1.05 ± 0.11 (9.9)	0.71 ± 0.18 (3.9)	AGN		Sy1 z=0.010254; V1432 Aql;
362	RX J1940-21025	295.051	-10.424	3.34 ± 0.18	2.35 ± 0.12	1.35 ± 0.20 (6.7)	CV	4	
363	NGC 6814	295.676	-10.329	4.17 ± 0.18	2.39 ± 0.12	2.82 ± 0.21	AGN	51	Sy1 z=0.005214;
364	IGR J19443+2117	296.006	21.306	0.93 ± 0.14 (6.6)	0.56 ± 0.09 (6.0)	0.38 ± 0.16 (2.4)	AGN?		=SWIFT J194353.0+212119; ↳
365	XTE J1946+274	296.410	27.366	5.38 ± 0.14	4.27 ± 0.10	0.91 ± 0.16 (5.7)	AGN		Sy2 z=0.0559; ↳
366	XSS J19459+4508	296.836	44.834	1.40 ± 0.16 (9.0)	0.72 ± 0.11 (6.8)	0.80 ± 0.16 (4.9)	AGN	34,27	2MASX J19471938+4449425; ↳ =IGR J19473+4452;
367	KS 1947+300	297.401	30.213	4.88 ± 0.14	3.00 ± 0.09	2.33 ± 0.15	HMXB		

Table 2. Continued.

Id	Name	RA [†] deg	Dec [‡] deg	F _{17–60 keV} [*] erg cm ⁻² s ⁻¹	F _{17–35 keV} [*] erg cm ⁻² s ⁻¹	F _{35–80 keV} [*] erg cm ⁻² s ⁻¹	Type	Ref. ^{**}	Notes ^{***}
				F _{17–60 keV} [*] erg cm ⁻² s ⁻¹	F _{17–35 keV} [*] erg cm ⁻² s ⁻¹	F _{35–80 keV} [*] erg cm ⁻² s ⁻¹			
368	3C403	298.086	2.515	1.23 ± 0.15 (7.9)	0.62 ± 0.10 (5.9)	1.00 ± 0.17 (5.8)	AGN	155	Sy2 z=0.059; Symbiotic X-ray binary;
369	4U1954+319	298.923	32.098	15.91 ± 0.13	11.05 ± 0.09	5.91 ± 0.14	LMXB		
370	Cyg X-1	299.589	35.203	965.98 ± 0.12	519.27 ± 0.08	674.58 ± 0.13	HMXB		Sy2 z=0.056146; =3C 405.0; =IGR J20006+3210;
371	Cygnus A	299.870	40.738	6.15 ± 0.12	3.53 ± 0.08	4.18 ± 0.12	AGN		Sy2 z=0.056146; =3C 405.0;
372	SWIFT J2000.6+3210	300.095	32.191	2.83 ± 0.12	1.79 ± 0.09	1.60 ± 0.13	HMXB	156	Sy2 z=0.056146; =3C 405.0;
373	IGR J20107+4534	302.643	45.568	0.68 ± 0.12 (5.5)	0.40 ± 0.09 (4.6)	<0.24			
374	IGR J20159+3713	303.881	37.188	1.20 ± 0.10	0.67 ± 0.07 (9.4)	0.72 ± 0.11 (6.6)	SNR		SNR G074.9+01.2; ↴ ↪=SWIFT J2015.9+3715; 2MASX J20183871+4041003; ↴ ↪=IGR J2018+4043; Sy2 z=0.0144;
375	IGR J20187+4041	304.641	40.685	1.78 ± 0.10	0.92 ± 0.07	1.13 ± 0.11	AGN	140,157	
376	IGR J20216+4359	305.427	43.991	0.83 ± 0.11 (7.7)	0.42 ± 0.08 (5.6)	0.67 ± 0.11 (6.3)	AGN	158	
377	IGR J20286+2544	307.136	25.736	3.21 ± 0.18	1.55 ± 0.12	2.69 ± 0.20	AGN	140,159	Sy2 z=0.014206; ↴ ↪ MCG +04-48-002;
378	EXO 2030+375	308.065	37.638	71.20 ± 0.10	41.69 ± 0.07	32.26 ± 0.10	HMXB		
379	Cyg X-3	308.108	40.960	167.45 ± 0.10	119.31 ± 0.07	57.55 ± 0.10	HMXB		Sy2 z=0.017; ↴ ↪ Quasar z=0.1735; =4C +21.55;
380	SWIFT J2033.4+2147	308.393	21.807	1.99 ± 0.26 (7.7)	1.01 ± 0.17 (5.8)	1.36 ± 0.29 (4.7)	AGN		
381	SWIFT J2037.2+4151	309.277	41.843	0.63 ± 0.10 (6.4)	0.51 ± 0.07 (7.5)	<0.20			
382	SWIFT J2044.0+2832	311.022	28.555	1.30 ± 0.17 (7.6)	0.85 ± 0.12 (7.2)	0.71 ± 0.18 (3.9)	AGN		Sy1 z=0.05; RX J2044.0+2833; 3A 2056+493; ↴ ↪ Blazar or microQSO;
383	IGR J20569+4940	314.172	49.657	1.00 ± 0.11 (8.9)	0.53 ± 0.08 (7.0)	0.49 ± 0.11 (4.2)	AGN	160	
384	SAX J2103.5+4545	315.898	45.751	9.80 ± 0.10	6.30 ± 0.07	4.19 ± 0.10	HMXB		
385	SWIFT J2113.5+5422	318.421	54.401	0.65 ± 0.13 (5.1)	0.44 ± 0.08 (5.1)	<0.27	CV	12	IRXS J211336.1+542226;
386	IGR J21178+5139	319.436	51.651	1.36 ± 0.12	0.65 ± 0.08 (8.3)	1.12 ± 0.12 (9.1)	AGN	140	2MASX J21175311+5139034;
387	IGR J21196+3333	319.899	33.552	1.10 ± 0.17 (6.4)	0.51 ± 0.12 (4.2)	0.87 ± 0.17 (5.1)	AGN	12	Sy1.5 z=0.051; ↴ ↪ IRXS J211928.4+3333259; ↪ V2069 Cyg;
388	IGR J21237+4218	320.932	42.301	1.27 ± 0.12	0.90 ± 0.08	0.35 ± 0.12 (3.0)	CV		
389	IGR J21247+5058	321.165	50.975	10.14 ± 0.12	5.48 ± 0.08	7.09 ± 0.12	AGN	60,133	Sy1 z=0.02; ↴ ↪ Sy1 z=0.014;
390	IGR J21277+5656	321.928	56.934	2.74 ± 0.14	1.73 ± 0.09	1.27 ± 0.15 (8.5)	CV	150	
391	IGR J21335+5105	323.434	51.129	3.65 ± 0.12	2.36 ± 0.08	1.59 ± 0.13	AGN	4	Sy1 z=0.02523; ↴ ↪ IRXS J213555.0+472823;
392	IGR J21358+4729	323.975	47.479	1.48 ± 0.12	0.75 ± 0.08 (9.4)	1.00 ± 0.12 (8.1)	AGN		
393	SS Cyg	325.692	43.580	3.72 ± 0.13	2.60 ± 0.09	1.29 ± 0.14 (9.3)	CV		
394	Cyg X-2	326.167	38.319	28.67 ± 0.18	25.34 ± 0.12	2.28 ± 0.18	LMXB		
395	BL Lac	330.663	42.272	1.56 ± 0.18 (8.4)	0.81 ± 0.12 (6.5)	1.25 ± 0.19 (6.4)	AGN		Blazar z=0.0688;
396	4U 2206+543	331.986	54.516	10.82 ± 0.13	6.71 ± 0.09	5.59 ± 0.15	HMXB	12	Sy1.5 z=0.112; ↴ ↪=IGR J22292+6647;
397	IGR J22292+6646	337.309	66.773	0.89 ± 0.13 (6.6)	0.60 ± 0.09 (6.7)	0.54 ± 0.14 (3.8)	AGN		2MASS J22295512+6243368;
398	IGR J22534+6243	343.365	62.723	0.60 ± 0.10 (5.8)	0.32 ± 0.07 (4.6)	0.25 ± 0.11 (2.3)	HMXB	161	
399	IGR J23206+6431	350.158	64.527	0.75 ± 0.09 (7.9)	0.36 ± 0.06 (5.8)	0.48 ± 0.10 (4.9)	AGN	158	
400	Cas A	350.847	58.810	4.91 ± 0.09	3.43 ± 0.06	2.21 ± 0.10	SNR	1	Sy2 z=0.037; ↴ ↪ USNO-A2.0 1575-05664433;
401	IGR J23308+7120	352.615	71.422	0.70 ± 0.14 (5.1)	0.41 ± 0.09 (4.5)	0.34 ± 0.14 (2.4)	AGN	158	Sy2 z=0.162; ↴ ↪=IGR J23524+5842;
402	IGR J23523+5844	358.075	58.759	0.70 ± 0.09 (7.8)	0.39 ± 0.06 (6.5)	0.66 ± 0.09 (7.0)	AGN		

Notes. ^(†) For the column description see Sect. 3. ^(‡) The positional accuracy of sources detected by IBIS/ISGRI depends on the source significance (Gros et al., 2003). The estimated 68% confidence intervals for sources detected at 5–6, 10, and $> 20\sigma$ are $2.1'$, $1.5'$, and $< 0.8'$, respectively (Krivonos et al., 2007b). ^(*) Source flux was measured in the nine-year time-averaged map. The flux measured with $\sigma < 4.7$ is highlighted in red. The flux measured at $S/N < 2\sigma$ is shown as an 2σ upper limit in red. If a detection significance does not exceed 10σ , it is shown in braces. Flux is expressed in units of $10^{-11} \text{ erg cm}^{-2} \text{s}^{-1}$. ^(**) (1) Masetti et al. (2008), (2) Den Hartog et al. (2005), (3) Bikmaev et al. (2006b), (4) Bikmaev et al. (2005), (5) Eckert et al. (2004), (6) Markwardt et al. (2004), (7) Kuiper et al. (2009), (9) Donato et al. (2005), (10) den Hartog et al. (2004b), (11) Bird et al. (2010), (12) Masetti et al. (2010b), (13) Kuiper et al. (2005), (14) Watson et al. (2009), (15) Baumgartner et al. (2010), (16) Parisi et al. (2012), (17) Lutovinov et al. (2012), (18) Lutovinov et al. (2008), (20) Burenin et al. (2008), (21) Krivonos et al. (2011), (22) Martí et al. (2004), (23) Reig & Roche (1999), (24) Torres et al. (2007), (25) Winter et al. (2008), (26) Bird et al. (2006), (27) Sazonov et al. (2005), (28) den Hartog et al. (2004a), (29) Masetti et al. (2006c), (30) Sazonov et al. (2008), (31) Revnivtsev et al. (2009), (32) Zurita Heras et al. (2009), (33) Kuiper et al. (2006a), (34) Revnivtsev et al. (2006), (35) Masetti et al. (2006d), (36) Moretti et al. (2006), (37) Masetti et al. (2010), (38) Leyder et al. (2008), (39) Fiocchi et al. (2010), (40) Bird et al. (2007), (41) Proust et al. (2004), (42) Tomsick et al. (2008), (43) Grebenev et al. (2004a), (44) Masetti et al. (2012), (46) Masetti et al. (2006e), (47) Chernyakova et al. (2005a), (48) Masetti et al. (2005), (49) Bassa et al. (2006), (50) Chernyakova et al. (2005b), (51) Tomsick et al. (2009), (52) Keek et al. (2006), (53) Renaud et al. (2010b), (54) Landi et al. (2011b), (55) Tueller et al. (2012), (56) Malizia et al. (2010), (57) Milišavljević et al. (2011), (58) Masetti et al. (2007b), (59) Landi et al. (2011a), (60) Walter et al. (2004), (61) Tomsick et al. (2007a), (63) Soldi et al. (2005), (64) Beckmann et al. (2005), (65) Kuiper et al. (2010), (66) Ratti et al. (2010), (67) Revnivtsev et al. (2003b), (68) Courvoisier et al. (2003), (69) Tomsick et al. (2003), (70) Lutovinov et al. (2005a), (71) Revnivtsev et al. (2003c), (72) Nespoli et al. (2010), (73) Bodaghee et al. (2006), (74) Tomsick et al. (2004), (75) Walter et al. (2006), (76) Lutovinov et al. (2004b), (77) Lutovinov et al. (2005b), (78) Molkov et al. (2003), (79) Chaty et al. (2008), (80) Grebenev et al. (2008a), (81) Nespoli et al. (2005b), (82) Hiemstra et al. (2011), (83) Lutovinov et al. (2010b), (84) Burenin et al. (2007), (85) Kalamkar et al. (2011), (86) Linares et al. (2009), (87) Churazov et al. (2007), (88) Degenaar et al. (2012), (89) Kuulkers et al. (2003), (90) Lutovinov & Revnivtsev (2003a), (91) Grebenev et al. (2005a), (92) Grebenev et al. (2007b), (93) Masetti et al. (2012a), (94) Bassani et al. (2005), (95) Brandt et al. (2005), (97) Lutovinov et al. (2004a), (98) Degenaar et al. (2010), (99) Kuulkers et al. (2006), (100) Gibaud et al. (2011), (101) Nucita et al. (2012), (102) Sunyaev et al. (2003a), (103) Smith & Hartigan (2006), (104) Kretschmar et al. (2004), (105) Heinke et al. (2009), (106) Bassani et al. (2004), (107) Torres et al. (2004), (108) Curran et al. (2011b), (109) Bélanger et al. (2006), (110) Krivonos et al. (2007a), (111) Revnivtsev et al. (2003a), (112) Brandt et al. (2006b), (113) Wijnands (2006), (114) Grebenev et al. (2005c), (115) Del Monte et al. (2008), (116) Revnivtsev et al. (2004a), (117) Meschederyakov et al. (2009), (118) Grebenev & Sunyaev (2007a), (119) Karasev et al. (2007a), (120) Karasev et al. (2010), (121) Soldi et al. (2006), (122) Paizis et al. (2007a), (123) Zolotukhin & Revnivtsev (2011), (124) Grebenev & Sunyaev (2004b), (125) Chelovekov & Grebenev (2007), (126) Sunyaev et al. (2003b), (127) in't Zand (2005), (128) Curran et al. (2011a), (129) Lutovinov et al. (2003c), (130) Brandt et al. (2007), (131) Revnivtsev et al. (2004), (133) Masetti et al. (2010), (132) Torrejón et al. (2004b), (134) Nucita et al. (2007), (135) Ubertini et al. (2005), (136) Funk et al. (2007), (137) Paizis et al. (2009), (138) Butler et al. (2009), (139) Markwardt (2008), (140) Bassani et al. (2009), (141) Bassani et al. (2006), (142) Lutovinov et al. (2003b), (143) Malizia et al. (2005), (144) Rodriguez et al. (2004), (145) Nespoli et al. (2008b), (146) Chernyakova et al. (2003), (147) Molkov et al. (2004), (148) Terrier et al. (2008), (149) Reynolds et al. (2012), (150) Bikmaev et al. (2006a), (151) Karasev et al. (2007b), (152) Hannikainen et al. (2003), (153) Steeghs et al. (2008), (154) Torres et al. (2006), (155) Masetti et al. (2007c), (156) Halpern (2006), (157) Gonçalves et al. (2008), (158) Bikmaev et al. (2008), (159) Masetti et al. (2010), (160) Landi et al. (2006b), (161) Masetti et al. (2012b), (****) The spatial confusion with the source XXX is indicated as CXXX. The measured flux of sources being in spatial confusion should be taken with the caution.